Table I. *Oligonucleotide primers and probes used for real-time PCR*

Target Gene	Type[a]	Primer or Probe (5′–3′)	Description (mer)
mTREM-1	F	CCAGAAGGCTTGGCAGAGACT	22
	B	ACTTCCCCATGTGGACTTCACT	22
mGAPDH	F	TGCAGTGGCAAAGTGGAGATT	21
	B	ATTTGCCGTGAGTGGAGTCAT	21
hTREM-1	F	GCCTTGTGCCCACTCTATACCA	22
	B	TGGAGACATCGGCAGTTGAC	20
	P	(FAM)CAGAACTGTGACCCAAGCTCCACCCA(TAMRA)	26
hsTREM-1	F	CCTCCCAAGGAGCCTCACA	19
	B	ACACCGGAACCCCTTGGT	18
	P	(FAM)CTGTTCGATCGCATCCGCTTGGT(TAMRA)	23

[a] F, forward primer; B, backward primer; and P, TaqMan Probe.

microbial inflammation. Therefore, we conducted this study to investigate the biological effects of PGE_2 on the expression and action of TREM-1.

Materials and Methods

Reagents

DI-004 (an EP1 agonist), AE1–259-01 (an EP2 agonist), AE-248 (an EP3 agonist), and AE1-329 (an EP4 agonist) were provided by Ono Pharmaceuticals. A monoclonal rat anti-mouse TREM-1 Ab and a monoclonal mouse anti-human TREM-1 Ab, as well as control mouse IgG1 and a polyclonal anti-actin Ab, were obtained from R&D Systems and Santa Cruz Biotechnology, respectively. HRP-conjugated rabbit anti-mouse IgG and HRP-conjugated rabbit anti-rat IgG were purchased from DakoCytomation. Specific ELISAs for human TNF-α and human IL-8 were obtained from BioSource International. 8-Bromoadenosine 3′, 5′ cyclic monophosphate (8-Br-cAMP), LPS, the MEK (MAPKK) inhibitor PD98059, the p38 MAPK inhibitor SB203580, and the PI3K inhibitor LY294002 were purchased from Sigma-Aldrich, while the protein kinase A (PKA) inhibitor H-89 was obtained from Seikagaku. PGD_2, PGE_2, 15-[1α, 2α(*Z*),3β(1*E*,3*S*),4α]-7-[3-[3-hydroxy-4-(4-iodophenoxy)-1-butenyl]-7-oxabicyclo[2.2.1]hept-2-yl]-5-heptenoic acid (I-BOP), a COX-1 inhibitor (SC560), a COX-2 inhibitor (NS398), and a PGE_2 EIA kit were obtained from Cayman Chemical.

Cell culture

Resident peritoneal macrophages (RPM) were isolated from male ICR mice (6–8 wk old) as reported elsewhere (15). Heparinized peripheral blood was obtained from healthy volunteers and human PBMC were isolated by density-gradient centrifugation with Ficoll-Paque. After washing with PBS, the RPM or PBMC were suspended in RPMI 1640 medium (Sigma-Aldrich) supplemented with 5% heat-inactivated FCS (HyClone), 100 U/ml penicillin, and 100 μg/ml streptomycin (Invitrogen Life Technologies) for culture under a 5% CO_2 atmosphere at 37°C.

RPM (1×10^6 cells) or PBMC (2×10^6 cells) were incubated for the indicated periods with or without various concentrations of PGs (PGD_2, PGE_2, I-BOP), 8-Br-cAMP, LPS, or E-series of prostaglandin (EP EP1–4) agonists. Then the expression of murine TREM-1 (mTREM-1), human TREM-1 (hTREM-1), and soluble hTREM-1 (hsTREM-1) was investigated.

RPM were incubated in the presence or absence of SC560 and/or NS398 for 1 h to inhibit endogenous COX activity, and then the cells were incubated in the presence of LPS for the indicated periods. To block protein kinase activity, RPM were incubated in the presence or absence of various inhibitors such as SB203580, PD98059, LY294002, or H89 for 30 min, after which the cells were incubated with LPS or PGE_2 for the indicated periods.

At the termination of incubation, cells and culture supernatants were obtained by centrifugation. Total RNA and protein were isolated by using RLT lysis buffer (Qiagen). Samples of cell lysate and culture medium were stored at −80°C until use.

Quantitative real-time PCR

Total RNA was extracted from cell lysates using an RNeasy Mini kit (Qiagen). The RNA was treated with DNase I (Qiagen) and cDNA was synthesized from 2 μg of random-primed total RNA in a volume of 20 μl using Omniscript reverse transcriptase (Qiagen). mTREM-1, GAPDH, and COX-2 were assessed by quantitative real-time PCR (SYBR) using specific oligonucleotide primers. hTREM-1, hsTREM-1, and rRNA were assessed by quantitative real-time PCR (TaqMan) using specific oligonucleotide primers and probe. hsTREM-1 was identified as a splice variant of hTREM-1 with a 193-base deletion (exon 3) from bases 471 to 663 (GenBank accession no. AF287008). To avoid amplification of hsTREM-1 mRNA, the forward primer for hTREM-1 was designed to fit exon 3 (the deletion site). To amplify only hsTREM-1, the backward primer was designed to hybridize to the 3′ end of exon 2 as well as the 5′ end of exon 4. These primers could specifically amplify hTREM-1 and hsTREM-1, respectively. The sequences of the primers and probes are listed in Table I. The rRNA primers and probe were purchased from Applied Biosystems. The SYBR PCR was performed in duplicate using a 25-μl reaction mixture containing 1 μl of cDNA, QuantiTect SYBR Green PCR (Qiagen), and 300 nM each of the sense and antisense primers. The PCR mixture was incubated for 15 min at 95°C, and then amplification was performed for 45 cycles, consisting of denaturation at 94°C for 15 s, annealing at 58°C for 30 s, and extension at 72°C for 30 s. TaqMan PCR was performed in duplicate with a 25-μl reaction mixture containing 1 μl of cDNA, 12.5 μl of QuantiTect Probe PCR (Qiagen), 400 nM each of the sense and antisense primers, and 200 nM of the probe. The PCR mixture was incubated for 15 min at 95°C to activate HotStarTaq DNA polymerase. Subsequently, amplification was performed for 45 cycles, consisting of denaturation at 94°C for 15 s and combined annealing extension at 59°C for 1 min. During the extension step, the ABI Prism 7700 Sequence Detection System monitored PCR amplification in real time by quantitative analysis of the emitted fluorescence. The amount of each sample mRNA was evaluated relative to the control sample, which was assigned a value of 1 arbitrary unit.

Western blot analysis

Culture medium or RPM (1×10^6 cells) was dissolved in sample buffer (350 mM Tris (pH 6.8), 10% SDS, 30% glycerol, 600 mM DTT, and 0.05% bromphenol blue), loaded onto 10% SDS-PAGE gel, and run at 20 mA for 1.5 h. Proteins in the supernatant were transferred to a polyvinylidene difluoride membrane (Roche Diagnostics) for 1.5 h at 200 mA by semidry blotting. The membrane was then blocked with 5% skim milk in PBS containing 0.05% Tween 20 for 1 h at 37°C, washed with PBS containing 0.1% Tween 20, and incubated overnight at 4°C with a monoclonal anti-human TREM-1 Ab (1 μg/ml). The blots were washed four times with TBS and incubated for 30 min with HRP-conjugated rabbit anti-mouse IgG. Immunoreactive bands were developed using a chemiluminescent substrate (ECL plus; Amersham Biosciences).

Assay of cytokine and chemokine production

Flat-bottom plates were precoated with 5 μg/ml of a monoclonal anti-human TREM-1 Ab or an isotype-matched control Ab (mouse IgG1) overnight at 4°C. After washing with PBS, PBMC (1×10^5 cells) were preincubated with or without PGE_2 (1 μM) for 5 h. Then the PBMC were added to the Ab-coated wells, and briefly spun in a centrifuge at 1200 rpm to bind TREM-1. After incubation for 24 h, culture medium was obtained by centrifugation and stored at −20°C until the levels of TNF-α and IL-8 in the supernatant were determined by specific ELISAs.

Assay of PGE_2 production

Concentration of PGE_2 in the culture supernatant was determined by using a PGE_2 EIA kit according to the manufacturer's instructions.

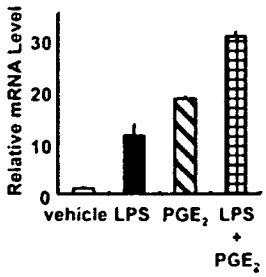

FIGURE 1. PGE_2 and LPS up-regulate mTREM-1 expression by RPM. RPM were incubated with or without PGE_2 (1 μM) for 1 h, and then were cultured in the presence or absence of LPS (100 ng/ml). The mTREM-1 mRNA level was determined by quantitative real-time PCR using murine GAPDH as the internal control. The relative level of mTREM-1 mRNA was evaluated by comparison with that in vehicle (EtOH)-treated RPM, which was defined as 1 arbitrary unit. Data are expressed as the mean ± SD of triplicate determinations.

Statistical analysis

Results are expressed as the mean ± SD. Statistical analysis was performed using the paired Student t test and $p < 0.05$ was considered to indicate significance.

Results

PGE_2 induces TREM-1 expression by RPM

PGE_2 is a mediator with a wide variety of biological effects in the process of microbial inflammation. To determine whether PGE_2 could influence the expression and action of TREM-1 in macrophages, RPM were pretreated with PGE_2 at a concentration of 1 μM for 1 h and then the cells were subsequently incubated in the presence or absence of LPS (100 ng/ml) for 1 h. Expression of mTREM-1 was determined by quantitative real-time PCR. LPS significantly increased expression of the *TREM-1* gene (Fig. 1), as previously reported. PGE_2 also caused significant induction of TREM-1 expression and the magnitude of gene expression was significantly higher in PGE_2-treated cells than in LPS-treated cells. Furthermore, a combination of PGE_2 and LPS caused additive enhancement of mTREM-1 expression by RPM.

To investigate the time course of PGE_2-induced expression of mTREM-1, RPM were incubated with 1 μM PGE_2 for the indicated periods. Induction of gene expression occurred quite rapidly and was observed as early as 1 h after stimulation, following declined for 12 h (Fig. 2*A*). RPM were incubated with varying concentrations of PGE_2 for 1 h to determine whether physiological levels of PGE_2 enhanced mTREM-1 expression. It was shown that PGE_2 increased mTREM-1 expression in a concentration-dependent manner. PGE_2 at a concentration as low as 10^{-10} M significantly induced mTREM-1 expression and maximal expression occurred after stimulation with 10^{-6}–10^{-7} M PGE_2 (Fig. 2*B*).

It has been demonstrated that monocytes and macrophages express various receptors for arachidonic acid metabolites, which are referred to EP, thromboxane-like prostanoid (TP), and CRTH2 (20). Therefore, we investigated the effects of specific ligands for these receptors on mTREM-1 expression by RPM. The cells were incubated for 1 h with PGE_2 (an EP receptor ligand), I-BOP (a TP receptor ligand), or PGD_2 (a CRTH2 ligand), and TREM-1 expression was evaluated by quantitative real-time PCR. PGE_2 induced TREM-1 expression, while neither I-BOP nor PGD_2 up-regulated mTREM-1 expression, indicating that PGE_2 was a specific inducer of mTREM-1 expression among these PGs (Fig. 2*C*).

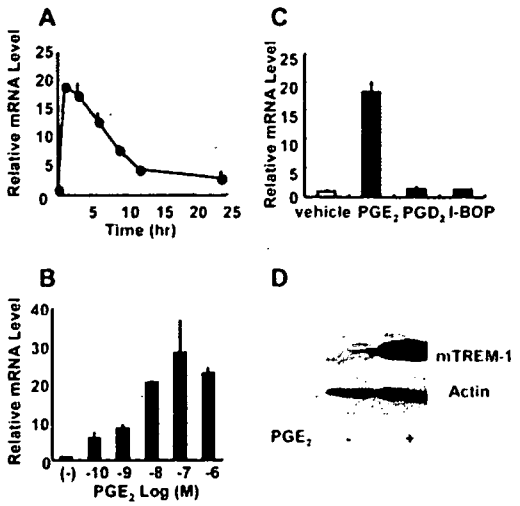

FIGURE 2. PGE_2 induces mTREM-1 expression in a time- or concentration-dependent manner. *A*, RPM were incubated with PGE_2 (1 μM) for the indicated periods and the mTREM-1 mRNA level was determined by quantitative real-time PCR. *B*, RPM were cultured with or without various concentrations of PGE_2 for 1 h and the mTREM-1 mRNA level was determined by quantitative real-time PCR. *C*, RPM were incubated with PGE_2 (1 μM), PGD_2 (1 μM), or I-BOP (0.2 μM) for 1 h and the mTREM-1 mRNA level was determined by quantitative real-time PCR. *D*, RPM were cultured with or without PGE_2 (1 μM) for 5 h, and expression of mTREM-1 protein and actin was determined by Western blot analysis. Data are expressed as the mean ± SD of triplicate determinations.

Western blot analysis using a specific anti-mouse TREM-1 mAb was performed to evaluate mTREM-1 protein expression by RPM after incubation with or without PGE_2 for 5 h. mTREM-1 protein was detected faintly when RPM were incubated with the vehicle alone, whereas increased expression of mTREM-1 was clearly seen when RPM were incubated with PGE_2 (10^{-6} M) for 5 h (Fig. 2*D*).

Endogenous PGE_2 induces TREM-1 expression by RPM

It has been demonstrated that LPS induces TREM-1 expression as well as the release of PGE_2 by macrophages (7–9, 21). To evaluate the possible influence of endogenous PGE_2 on LPS-induced mTREM-1 expression, RPM were stimulated with LPS (100 ng/ml) for the indicated periods, after which PGE_2 production and *mTREM-1* gene expression were determined by EIA and quantitative real-time PCR, respectively. PGE_2 synthesis gradually increased up to 4 h, and then the maximum level was maintained

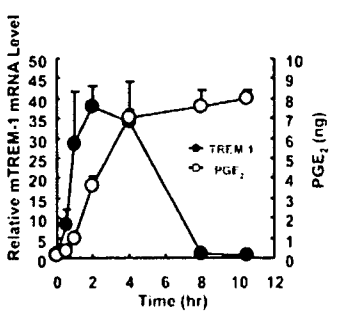

FIGURE 3. LPS-induced PGE_2 production up-regulates mTREM-1 expression by RPM. RPM were stimulated with LPS (100 ng/ml) for the indicated periods. Then the mTREM-1 mRNA level was determined by quantitative real-time PCR, and PGE_2 synthesis was determined by using a PGE_2 EIA kit. Data are expressed as the mean ± SD of triplicate determinations.

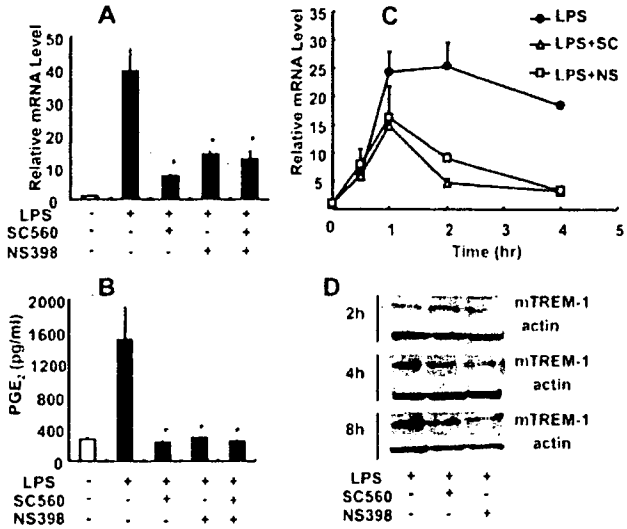

FIGURE 4. Effect of COX inhibitors on LPS-induced mTREM-1 expression by RPM. RPM were pretreated with or without SC560 and/or NS398 for 1 h, and were subsequently incubated in the presence or absence of LPS (100 ng/ml) for the indicated periods. *A*, The mTREM-1 mRNA level at 2 h after LPS stimulation was determined by quantitative real-time PCR. *B*, PGE_2 synthesis at 2 h after LPS stimulation was determined by a PGE_2 EIA kit. *C*, Time course of mTREM-1 mRNA expression was determined by quantitative real-time PCR. *D*, mTREM-1 protein and actin was determined by Western blot analysis. Data are expressed as the mean ± SD of triplicate determinations. *, $p < 0.01$, vs LPS-stimulated RPM by Student's unpaired *t* test.

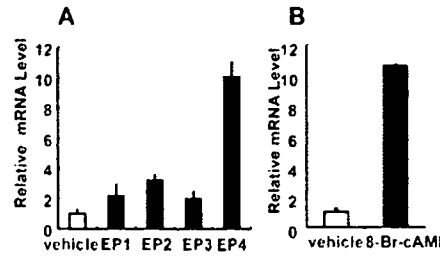

FIGURE 5. Enhancement of mTREM-1 expression by an EP4 agonist and cAMP analog. *A*, RPM were incubated with or without agonists for EP1 to EP4 agonists (1 μM) for 1 h and the mTREM-1 mRNA level was determined by quantitative real-time PCR. *B*, RPM were incubated with or without 8-Br-cAMP (0.5 mM) for 1 h. Data are expressed as the mean ± SD of triplicate determinations.

until 11 h after stimulation (Fig. 3). In contrast, gene expression of mTREM-1 occurred quite rapidly and was seen as early as 0.5 h after stimulation when PGE_2 production was not detected. Maximum induction of mTREM-1 was observed at 2–4 h after stimulation and gene expression returned to the basal level by 8 h. These findings indicated that PGE_2 synthesis did not precede the induction of *mTREM-1* gene expression.

mTREM-1 expression was significantly induced by a physiological concentration of PGE_2. Therefore, the regulatory roles of PGE_2 on TREM-1 expression was investigated. Because PGE_2 synthesis is regulated by COX-1 and COX-2, RPM were incubated for 1 h in the presence or absence of SC560 (a selective COX-1 inhibitor) or NS398 (a selective COX-2 inhibitor), and then the cells were stimulated with LPS for 2 h. mTREM-1 expression and PGE_2 synthesis was determined by quantitative real-time PCR and EIA, respectively. Both inhibitors for COX-1 and COX-2 partially, but significantly, inhibited LPS-induced expression of mTREM-1 (Fig. 4*A*). When the effects of COX inhibitors on PGE_2 synthesis by LPS-stimulated RPM were investigated, these inhibitors also suppressed PGE_2 synthesis (Fig. 4*B*). Vehicle (DMSO) did not affect on LPS-induced PGE_2 synthesis and mTREM-1 expression (data not shown).

To investigate the effect of PGE_2 on LPS-induced mTREM-1 mRNA expression at early time points, RPM were stimulated with LPS in the presence or absence of COX inhibitors for the indicated periods. Both COX-1 and COX-2 inhibitors failed to inhibit mTREM-1 expression at 0.5 h after LPS stimulation, whereas mTREM-1 expression at 1 h was partially inhibited, and that at 2 and 4 h was significantly abolished by COX inhibitors (Fig. 4*C*). These findings indicated that the effect of PGE_2 on LPS-induced mTREM-1 expression was predominant at late time points (>2 h after stimulation) but not at early time points (0.5 and 1 h after stimulation).

After RPM were incubated with LPS in the presence or absence of COX inhibitors for various times, the expression of mTREM-1 protein was determined by Western blot analysis. Both inhibitors reduced LPS-induced TREM-1 expression at 4 and 8 h but not at 2 h after stimulation (Fig. 4*D*). Actin as the internal control was similarly detected in all samples. These findings indicated that LPS-induced expression of mTREM-1 on RPM was at least partly promoted by endogenous PGE_2.

PGE_2-induced TREM-1 expression is mediated by the EP4 receptor and cAMP

It has been shown that the biological functions of PGE_2 are mediated by four specific receptors, which are coupled to G-protein and are referred to as EP1 to EP4 (20). To determine which EP receptors mediated PGE_2-induced mTREM-1 expression, RPM were incubated with four synthetic agonists specific for each of the EP receptors (each at a concentration of 1 μM), and then mTREM-1 expression was evaluated by quantitative real-time PCR. The EP4 agonist significantly up-regulated TREM-1 expression in RPM, whereas the EP1, EP2, and EP3 agonists failed to enhance TREM-1 expression (Fig. 5*A*).

Activation of the EP4 receptor enhances intracellular accumulation of cAMP via adenylate cyclase. Therefore, we examined the influence of 8-Br-cAMP (a stable cAMP analog) on mTREM-1 expression by RPM. Treatment of RPM with 8-Br-cAMP at a concentration of 5×10^{-4} M for 1 h significantly enhanced expression of the *mTREM-1* gene by RPM (Fig. 5*B*). EP4 agonist and 8-Br-cAMP also induced TREM-1 mRNA expression in J774.1 and PBMC (data not shown). These finding clearly suggested that PGE_2-induced TREM-1 expression on RPM was related to EP4 receptor- and cAMP-mediated signaling.

Blocking of PKA, p38 MAPK, and PI3K inhibits PGE_2-induced mTREM-1 expression

Intracellular cAMP is a major regulator of PKA (22) and cAMP also activates the PI3K-, p38 MAPK-, and ERK-signaling pathways (23–25). Therefore, we investigated the signaling pathways involved in PGE_2-induced expression of TREM-1 by using synthetic inhibitors of these kinases. A PKA inhibitor (H89), a p38 MAPK inhibitor (SB203580), and a PI3K inhibitor (LY294002) significantly suppressed PGE_2-induced TREM-1 expression, whereas a MAPKK inhibitor (PD98059) failed to influence TREM-1 expression (Fig. 6). Inhibitory effects of these inhibitors were observed in a dose- or time-dependent manner (data not shown). These results suggested that PGE_2-induced TREM-1 expression was mediated via the PKA, PI3K, and p38 MAPK pathways.

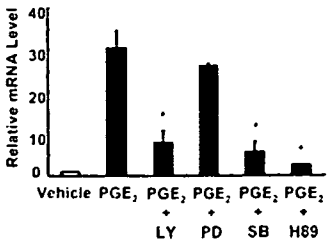

FIGURE 6. Inhibition of PKA, p38 MAPK, or PI3K suppresses PGE_2-induced mTREM-1 expression by RPM. RPM were pretreated with or without LY294002 (20 μM), PD98059 (30 μM), SB203580 (20 μM) H-89 (20 μM) for 30 min, and then were incubated with PGE_2 (1 μM) for 1 h. The mTREM-1 mRNA level was determined by quantitative real-time PCR. Data are expressed as the mean ± SD of triplicate determinations. *, $p < 0.01$ vs PGE_2-stimulated RPM by Student's unpaired t test.

Activation of TREM-1 significantly enhances cytokine production by PGE_2-treated PBMC

An agonistic anti-TREM-1 mAb has been shown to stimulate the production of proinflammatory cytokines by monocytes (1, 7, 9). It was difficult to transfer PGE_2-treated RPM to Ab-coated wells, because the cells tightly adhere to the culture dishes. Therefore, PBMC were used to determine whether TREM-1 could enhance cytokine production by PGE_2-treated monocytes. Cells were incubated in the presence or absence of PGE_2 (10^{-6} M) for 5 h, and then harvested for incubation in agonistic anti-TREM-1 mAb-coated wells for 24 h. Then the levels of TNF-α and IL-8 in the culture supernatant were determined by specific ELISAs. The agonistic anti-TREM-1 mAb caused a significant increase of TNF-α production by PGE_2-pretreated PBMC (Fig. 7*A*). Production of TNF-α by PGE_2-treated cells was 6-fold higher than that by untreated cells. The agonistic anti-TREM-1 mAb also increased IL-8 production by PGE_2-pretreated PBMC and the magnitude of this enhancement was 4.6-fold (Fig. 7*B*). These results indicated that

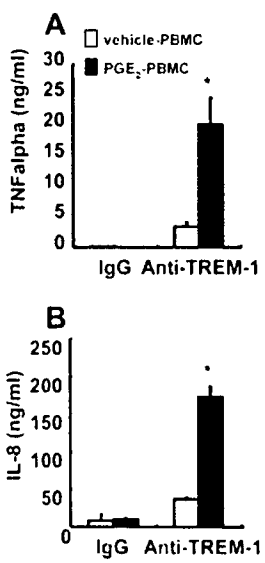

FIGURE 7. An agonistic anti-TREM-1 mAb enhances the production of proinflammatory cytokines by PGE_2-pretreated PBMC. PBMC were incubated with or without PGE_2 for 5 h, and then the cells were incubated in the presence or absence of the agonistic anti-TREM-1 mAb (5 μg/ml) or an isotype control Ab (5 μg/ml) for 24 h. Production of TNF-α (*A*) and IL-8 (*B*) was determined by specific ELISAs. Data are expressed as the mean ± SD of triplicate determinations. *, $p < 0.01$ vs vehicle-stimulated PBMC by Student's unpaired t test.

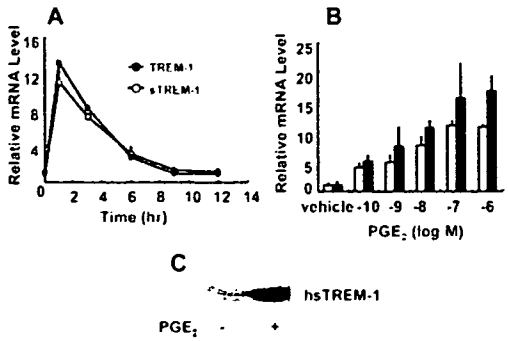

FIGURE 8. PGE_2 induces hTREM-1 and hsTREM-1 expression by PBMC in a time- and concentration-dependent manner. *A*, PBMC were incubated with PGE_2 (1 μM) for the indicated periods. Expression of the *hTREM-1* gene (○) and the *hsTREM-1* gene (●) was determined by real-time quantitative PCR. *B*, PBMC were cultured with or without various concentrations of PGE_2 for 1 h. Then the hTREM-1 (□) and hsTREM-1 (■) mRNA levels were determined by real-time quantitative PCR. *C*, PBMC were incubated with or without PGE_2 (1 μM) for 5 h and hsTREM-1 protein in the same volume of the supernatant (20 μl) was determined by Western blot analysis. Data are expressed as the mean ± SD of triplicate determinations.

TREM-1 induced by PGE_2 was functional and enhanced the production of proinflammatory cytokines by PBMC.

PGE_2 induces hTREM-1 and hsTREM-1 expression by PBMC

It has been demonstrated that human monocytes are capable of expressing sTREM-1 as well as the cell surface form (3–5). Although sTREM-1 has also been identified in mice, the precise structure and function of soluble mTREM-1 are not yet known. Therefore, we investigated the expression of hTREM-1 and hsTREM-1 by PGE_2-treated PBMC to evaluate which type was predominantly expressed. After PBMC were incubated with PGE_2, *hTREM-1* and *hsTREM-1* gene expression were separately determined by quantitative real-time PCR.

Induction of both *hTREM-1* and *hsTRM-1* gene expression occurred quite rapidly and was seen as early as 1 h after stimulation, a subsequent declined until 9 h (Fig. 8*A*). To determine whether physiological concentrations of PGE_2 could induce the expression of hTREM-1 and hsTREM-1, PBMC were incubated with various concentrations of PGE_2 for 1 h and gene expression was determined. It was found that PGE_2 promoted both hTREM-1 and hsTREM-1 expression in a concentration-dependent manner, with maximal expression occurring at 10^{-6} or 10^{-7} M (Fig. 8*B*).

Western blot analysis using a specific anti-human TREM-1 mAb was performed to detect sTREM-1 protein. PBMC were incubated with or without PGE_2 for 5 h, and then the sTREM-1 protein level in the culture supernatant was determined by Western blotting. sTREM-1 was detected at very low levels when PBMC were incubated with the vehicle alone, whereas sTREM-1 expression was increased when PBMC were incubated with PGE_2 for 5 h (Fig. 8*C*). Taken together, these findings showed that PGE_2 up-regulated the expression of hTREM-1 as well as hsTREM-1 by monocytes.

Discussion

The present study provided evidence that PGE_2 up-regulates mTREM-1 expression by RPM, as well as hTREM-1 and hsTREM-1 expression by human PBMC. LPS-induced TREM-1 expression is at least partly regulated by endogenous PGE_2, because COX inhibitors significantly reduced TREM-1 expression. PGE_2-induced TREM-1 expression was mediated by EP-4, cAMP, and various kinases such as PKA, PI3K, and p38 MAPK. PGE_2-induced TREM-1 was functional,

because agonistic anti-TREM-1 mAb promoted a significant increase in the production of TNF-α and IL-8.

It is known that TREM-1 is specifically up-regulated by microbial products such as LPS, lipoteichoic acid (LTA), or zymosan (1, 7, 9, 26). However, the present study provided the first demonstration that PGE_2 could induce TREM-1 expression by both RPM and PBMC. Induction of TREM-1 expression by PGE_2 was also observed in a human monocyte cell line (U937) and a murine macrophage cell line (J774.1) (data not shown), indicating that PGE_2 is an inducer of TREM-1 expression by both monocytes and macrophages. PGE_2 was a specific regulator of mTREM-1 expression, because specific ligands for the CRTH2 and TP receptors (which are expressed on macrophages) failed to induce mTREM-1 expression. Biological effect of endogenous PGE_2 on TREM-1 expression was predominant in the late phase of LPS-induced TREM-1 expression. This is based on the findings that COX inhibitors abrogated mTREM-1 expression after 2 h and also reduced mTREM-1 protein expression after 4–8 h following LPS stimulation.

In the present study, both COX-1 and COX-2 inhibitors suppressed PGE_2 synthesis and TREM-1 induction. It has been documented that LPS promoted PGE_2 production through the induction and activation of the COX-2, but not COX-1 (21, 27). However, Rouzer et al. (21) also reported that SC560 (COX-1 inhibitor) inhibits PG synthesis through inhibition of COX-2 as well as COX-1 in LPS-stimulated RPM. Because this cross-inhibition was not observed in other cells, it appeared to be specific in RPM. TNF-α is also an inducer of PGE_2 synthesis, but a previous study demonstrated that TNF-α had a limited effect on TREM-1 expression (7, 28). The reasons for this difference are not known, but it might be related to different mechanisms of action on monocytes and macrophages.

EP4, one of the receptors for PGE_2, increases intracellular cAMP levels via activation of adenylate cyclase and promotes activation of the PKA, PI3K, p38 MAPK, and MAPKK pathways (22–25). The present study demonstrated that a specific EP4 agonist and 8-Br-cAMP both enhanced *mTREM-1* gene expression, while inhibitors of PKA, p38 MAPK, and PI3K blocked the PGE_2-induced increase of mTREM-1 expression. These findings suggested that PGE_2-induced up-regulation of mTREM-1 expression was mediated by the binding of PGE_2 to EP4, which was followed by accumulation of cAMP and activation of various kinases, including PKA, p38 MAPK, and PI3K. This is consistent with the findings of previous studies demonstrating that PGE_2 potentially activate various kinases such as PKA, PI3K, and p38 MAPK independently (29, 30). COX inhibitors failed to completely suppress LPS-induced up-regulation of mTREM-1 expression by RPM, and these inhibitors abolished TREM-1 expression only in the late phase, but not early phase of LPS stimulation. These indicate that other pathways might also be involved in the induction of TREM-1 expression by LPS. Knapp et al. (28) recently demonstrated that a PI3K-dependent pathway played a central role, while MAPK also played a limited role, in LPS-induced up-regulation of TREM-1 expression by monocytes. Several signaling pathways might be involved in LPS-induced TREM-1 expression, and the endogenous PGE_2-mediated pathway seems to be one of the mechanisms of LPS-induced TREM-1 expression on monocytes and macrophages.

TLR and TREM-1 cooperate to induce an inflammatory response, because activation of TREM-1 causes a marked increment in the production of proinflammatory cytokines by macrophages when LPS is used as the costimulus (1, 8, 9). TREM-1 activates a downstream signaling pathway through DAP12, which involves tyrosine phosphorylation, activation of mitogen-activated protein kinases, and mobilization of Ca^{2+}. In contrast, TLRs directly recognize certain microbial products and components, such as LPS, LTA, and bacterial DNA. MyD88, IRAK, TRAF6, and IKK are essentially involved in the TLR-signaling pathway. These kinases can potentially induce the production of proinflammatory cytokines via the activation of NF-κB (31). Natural ligands for TREM-1 remain to be identified. If specific ligands for TREM-1 are located at the foci of microbe-induced inflammation, interactions between TREM-1 and TLRs can synergistically induce inflammatory responses. In this case, cooperation between TLRs and TREM-1 could occur at several levels during the process of LPS-induced inflammation. The present study showed that an LPS-induced increase in the production of PGE_2 promoted TREM-1 expression, and activation of TREM-1 on PGE_2-treated PBMC enhanced the production of proinflammatory cytokines. Based on these findings, we hypothesized that PGE_2-induced up-regulation of TREM-1 expression may play an important role in enhancing the TLR-mediated response of macrophages to LPS stimulation.

Several line of evidence indicated that decoy receptors can modulate inflammatory responses by blocking the action by agonists (32, 33). sTREM-1 is a natural decoy receptor that could potentially inhibit TREM-1-mediated activation of cells through competition with natural ligand(s) for receptor binding. Synthetic sTREM-1 has been shown to inhibit LPS-induced cytokine production by monocytes in vitro (6). Furthermore, a recombinant sTREM-1 fusion protein and synthetic soluble TREM-1 have been shown to protect mice against lethal LPS challenge or bacterial sepsis by suppressing inflammatory cytokine production (6, 9). In contrast, it has been demonstrated that PGE_2 can suppress the production of various cytokines (such as TNF-α, IL-8, MCP-1, IFN-γ-inducible protein-10, and MIP-1β) by LPS-stimulated macrophages through EP2- and/or EP4-mediated pathways (34, 35). PGE_2 also induces the production of IL-10, which can have an anti-inflammatory effect (36). Present study demonstrated that PGE_2 induced the release of sTREM-1 by PBMC. Therefore, PGE_2 might suppress inflammation not only by inhibiting the production of proinflammatory cytokines, but also by inducing expression of the decoy receptor sTREM-1 and increasing the production of IL-10. However, activation of TREM-1 on PGE_2-treated PBMC enhanced the production of proinflammatory cytokines, indicating that PGE_2 may exert bidirectional effects on monocytes and macrophages to modulate inflammation through altering the expression of TREM-1 and sTREM-1.

Blocking of PGs has been shown to increase LPS-induced cytokine production both in vitro and in vivo (36–39). This is consistent with the previous finding that PGE_2 and EP4 agonists attenuated LPS-induced cytokine production in mice (40). However, a number of studies have provided evidence that COX inhibitors can improve survival after the onset of endotoxic shock and COX-deficient mice are resistant to endotoxin-induced inflammation and death (17, 19, 41). Thus, the precise pathophysiological role of PGE_2 in microbe infection still remains undefined. Further investigations should be directed toward the in vivo effects of PGE_2-induced TREM-1 and sTREM-1 in sepsis models.

Increased expression of TREM-1 has been observed at sites of inflammation caused by microbial pathogens (9). However, we recently demonstrated that monosodium urate monohydrate (MSU) crystals induced mTREM-1 expression in monocytes and macrophages in vitro and in vivo (42), indicating that TREM-1 might be involved in the development of acute gouty arthritis. We also observed that MSU crystal-induced mTREM-1 expression is regulated, at least in part, by endogenous produced PGE_2 (our unpublished data). These findings suggest the possibility that PGE_2 might enhance TREM-1 expression in nonmicrobial inflammatory diseases including acute gouty arthritis. If a natural TREM-1 ligand is also induced in nonmicrobial inflammation, it could enhance inflammatory responses by activating PGE_2-induced

TREM-1. Furthermore, nonmicrobial products such as heat shock protein 60, which are induced in various inflammatory diseases, have been shown to stimulate TLRs (43). Thus, it is presumed that activation of PGE_2-induced TREM-1 and TLRs by specific ligands might cooperatively increase the inflammatory responses in patients with nonmicrobial inflammatory diseases.

The present study provided a first evidence that PGE_2 induces the expression of both TREM-1 and sTREM-1 by macrophages. This finding sheds new light on the role of PGE_2 as a regulator of the inflammatory response to microbial infection. Further investigations should be directed toward the assessment of pathophysiological roles of TREM-1 and sTREM-1 in various inflammatory diseases. Such studies may help to elucidate the precise role of PGE_2-induced TREM-1 expression in inflammation and could possibly provide evidence leading to new strategies for the treatment of inflammatory diseases.

Acknowledgments

We thank Rie Hasegawa and Mitsuko Mizuno for their technical support.

Disclosures

The authors have no financial conflict of interest.

References

1. Bouchon, A., J. Dietrich, and M. Colonna. 2000. Inflammatory responses can be triggered by TREM-1, a novel receptor expressed on neutrophils and monocytes. *J. Immunol.* 164: 4991–4995.
2. Colonna, M., and F. Facchetti. 2003. TREM-1 (triggering receptor expressed on myeloid cells): a new player in acute inflammatory responses. *J. Infect. Dis.* 187: S397–S401.
3. Allaouchiche, B., and E. Boselli. 2004. Soluble TREM-1 and the diagnosis of pneumonia. *N. Engl. J. Med.* 350: 1904–1905.
4. Gibot, S., M. N. Kolopp-Sarda, M. C. Bene, A. Cravoisy, B. Levy, G. C. Faure, and P. E. Bollaert. 2004. Plasma level of a triggering receptor expressed on myeloid cells-1: its diagnostic accuracy in patients with suspected sepsis. *Ann. Intern. Med.* 141: 9–15.
5. Gingras, M. C., H. Lapillonne, and J. F. Margolin. 2002. TREM-1, MDL-1, and DAP12 expression is associated with a mature stage of myeloid development. *Mol. Immunol.* 38: 817–824.
6. Gibot, S., M. N. Kolopp-Sarda, M. C. Bene, P. E. Bollaert, A. Lozniewski, F. Mory, B. Levy, and G. C. Faure. 2004. A soluble form of the triggering receptor expressed on myeloid cells-1 modulates the inflammatory response in murine sepsis. *J. Exp. Med.* 200: 1419–1426.
7. Bleharski, J. R., V. Kiessler, C. Buonsanti, P. A. Sieling, S. Stenger, M. Colonna, and R. L. Modlin. 2003. A role for triggering receptor expressed on myeloid cells-1 in host defense during the early-induced and adaptive phases of the immune response. *J. Immunol.* 170: 3812–3818.
8. Colonna, M. 2003. TREMs in the immune system and beyond. *Nat. Rev. Immunol.* 3: 445–453.
9. Bouchon, A., F. Facchetti, M. A. Weigand, and M. Colonna. 2001. TREM-1 amplifies inflammation and is a crucial mediator of septic shock. *Nature* 410: 1103–1107.
10. Marnett, L. J., S. W. Rowlinson, D. C. Goodwin, A. S. Kalgutkar, and C. A. Lanzo. 1999. Arachidonic acid oxygenation by COX-1 and COX-2: mechanisms of catalysis and inhibition. *J. Biol. Chem.* 274: 22903–22906.
11. Bertelsen, L. S., G. Paesold, L. Eckmann, and K. E. Barrett. 2003. *Salmonella* infection induces a hypersecretory phenotype in human intestinal xenografts by inducing cyclooxygenase 2. *Infect. Immun.* 71: 2102–2109.
12. Lopez-Urrutia, L., A. Alonso, Y. Bayon, M. L. Nieto, A. Orduna, and M. Sanchez Crespo. 2001. *Brucella* lipopolysaccharides induce cyclooxygenase-2 expression in monocytic cells. *Biochem. Biophys. Res. Commun.* 289: 372–375.
13. Anderson, F. L., W. Jubiz, T. J. Tsagaris, and H. Kuida. 1975. Endotoxin-induced prostaglandin E and F release in dogs. *Am. J. Physiol.* 228: 410–414.
14. Kessler, E., R. C. Hughes, E. N. Bennett, and S. M. Nadela. 1973. Evidence for the presence of prostaglandin-like material in the plasma of dogs with endotoxin shock. *J. Lab. Clin. Med.* 81: 85–94.
15. Strassmann, G., V. Patil-Koota, F. Finkelman, M. Fong, and T. Kambayashi. 1994. Evidence for the involvement of interleukin 10 in the differential deactivation of murine peritoneal macrophages by prostaglandin E_2. *J. Exp. Med.* 180: 2365–2370.
16. Portanova, J. P., Y. Zhang, G. D. Anderson, S. D. Hauser, J. L. Masferrer, K. Seibert, S. A. Gregory, and P. C. Isakson. 1996. Selective neutralization of prostaglandin E_2 blocks inflammation, hyperalgesia, and interleukin 6 production in vivo. *J. Exp. Med.* 184: 883–891.
17. Wise, W. C., J. A. Cook, T. Eller, and P. V. Halushka. 1980. Ibuprofen improves survival from endotoxic shock in the rat. *J. Pharmacol. Exp. Ther.* 215: 160–164.
18. Shoup, M., L. K. He, H. Liu, R. Shankar, and R. Gamelli. 1998. Cyclooxygenase-2 inhibitor NS-398 improves survival and restores leukocyte counts in burn infection. *J. Trauma* 45: 215–220.
19. Jacobs, E. R., M. E. Soulsby, R. C. Bone, F. J. Wilson, Jr., and F. C. Hiller. 1982. Ibuprofen in canine endotoxin shock. *J. Clin. Invest.* 70: 536–541.
20. Tilley, S. L., T. M. Coffman, and B. H. Koller. 2001. Mixed messages: modulation of inflammation and immune responses by prostaglandins and thromboxanes. *J. Clin. Invest.* 108: 15–23.
21. Rouzer, C. A., P. J. Kingsley, H. Wang, H. Zhang, J. D. Morrow, S. K. Dey, and L. J. Marnett. 2004. Cyclooxygenase-1-dependent prostaglandin synthesis modulates tumor necrosis factor-α secretion in lipopolysaccharide-challenged murine resident peritoneal macrophages. *J. Biol. Chem.* 279: 34256–34268.
22. Taylor, S. S., J. Yang, J. Wu, N. M. Haste, E. Radzio-Andzelm, and G. Anand. 2004. PKA: a portrait of protein kinase dynamics. *Biochim. Biophys. Acta* 1697: 259–269.
23. Cass, L. A., S. A. Summers, G. V. Prendergast, J. M. Backer, M. J. Birnbaum, and J. L. Meinkoth. 1999. Protein kinase A-dependent and -independent signaling pathways contribute to cyclic AMP-stimulated proliferation. *Mol. Cell Biol.* 19: 5882–5891.
24. Fiebich, B. L., S. Schleicher, O. Spleiss, M. Czygan, and M. Hull. 2001. Mechanisms of prostaglandin E_2-induced interleukin-6 release in astrocytes: possible involvement of EP4-like receptors, p38 mitogen-activated protein kinase and protein kinase C. *J. Neurochem.* 79: 950–958.
25. Busca, R., P. Abbe, F. Mantoux, E. Aberdam, C. Peyssonnaux, A. Eychene, J. P. Ortonne, and R. Ballotti. 2000. Ras mediates the cAMP-dependent activation of extracellular signal-regulated kinases (ERKs) in melanocytes. *EMBO J.* 19: 2900–2910.
26. Nochi, H., N. Aoki, K. Oikawa, M. Yanai, Y. Takiyama, Y. Atsuta, H. Kobayashi, K. Sato, M. Tateno, T. Matsuno, et al. 2003. Modulation of hepatic granulomatous responses by transgene expression of DAP12 or TREM-1-Ig molecules. *Am. J. Pathol.* 162: 1191–1201.
27. Gray, T., P. Nettesheim, C. Loftin, J. S. Koo, J. Bonner, S. Peddada, and R. Langenbach. 2004. Interleukin-1β-induced mucin production in human airway epithelium is mediated by cyclooxygenase-2, prostaglandin E_2 receptors, and cyclic AMP-protein kinase A signaling. *Mol. Pharmacol.* 66: 337–346.
28. Knapp, S., S. Gibot, A. de Vos, H. H. Versteeg, M. Colonna, and T. van der Poll. 2004. Expression patterns of surface and soluble triggering receptor expressed on myeloid cells-1 in human endotoxemia. *J. Immunol.* 173: 7131–7134.
29. Fujino, H., S. Salvi, and J. W. Regan. 2005. Differential regulation of phosphorylation of the cAMP response element-binding protein after activation of EP2 and EP4 prostanoid receptors by prostaglandin E_2. *Mol. Pharmacol.* 68: 251–259.
30. Caristi, S., G. Piraino, M. Cucinotta, A. Valenti, S. Loddo, and D. Teti. 2005. Prostaglandin E_2 induces interleukin-8 gene transcription by activating C/EBP homologous protein in human T lymphocytes. *J. Biol. Chem.* 280: 14433–14442.
31. Takeda, K., and S. Akira. 2005. Toll-like receptors in innate immunity. *Int. Immunol.* 17: 1–14.
32. Arend, W. P. 1991. Interleukin 1 receptor antagonist: a new member of the interleukin 1 family. *J. Clin. Invest.* 88: 1445–1451.
33. Abramson, S. B., and A. Amin. 2002. Blocking the effects of IL-1 in rheumatoid arthritis protects bone and cartilage. *Rheumatology* 41: 972–980.
34. Takayama, K., G. Garcia-Cardena, G. K. Sukhova, J. Comander, M. A. Gimbrone, Jr., and P. Libby. 2002. Prostaglandin E_2 suppresses chemokine production in human macrophages through the EP4 receptor. *J. Biol. Chem.* 277: 44147–44154.
35. Treflkorn, L., R. Scheibe, T. Maruyama, and P. Dieter. 2004. PGE_2 exerts its effect on the LPS-induced release of TNF-α, ET-1, IL-1α, IL-6 and IL-10 via the EP2 and EP4 receptor in rat liver macrophages. *Prostaglandins Other Lipid Mediat.* 74: 113–123.
36. Dong, Y. L., D. N. Herndon, T. Z. Yan, and J. P. Waymack. 1993. Blockade of prostaglandin products augments macrophage and neutrophil tumor necrosis factor synthesis in burn injury. *J. Surg. Res.* 54: 480–485.
37. Ertel, W., M. H. Morrison, P. Wang, Z. F. Ba, A. Ayala, and I. H. Chaudry. 1991. The complex pattern of cytokines in sepsis: association between prostaglandins, cachectin, and interleukins. *Ann. Surg.* 214: 141–148.
38. Sacco, S., D. Agnello, M. Sottocorno, G. Lozza, A. Monopoli, P. Villa, and P. Ghezzi. 1998. Nonsteroidal anti-inflammatory drugs increase tumor necrosis factor production in the periphery but not in the central nervous system in mice and rats. *J. Neurochem.* 71: 2063–2070.
39. Sironi, M., M. Gadina, M. Kankova, F. Riganti, A. Mantovani, M. Zandalasini, and P. Ghezzi. 1992. Differential sensitivity of in vivo TNF and IL-6 production to modulation by anti-inflammatory drugs in mice. *Int. J. Immunopharmacol.* 14: 1045–1050.
40. Sakamoto, A., J. Matsumura, S. Mii, Y. Gotoh, and R. Ogawa. 2004. A prostaglandin E_2 receptor subtype EP4 agonist attenuates cardiovascular depression in endotoxin shock by inhibiting inflammatory cytokines and nitric oxide production. *Shock* 22: 76–81.
41. Ejima, K., M. D. Layne, I. M. Carvajal, P. A. Kritek, R. M. Baron, Y. H. Chen, J. Vom Saal, B. D. Levy, S. F. Yet, and M. A. Perrella. 2003. Cyclooxygenase-2-deficient mice are resistant to endotoxin-induced inflammation and death. *FASEB J.* 17: 1325–1327.
42. Murakami, Y., T. Akahoshi, I. Hayashi, H. Endo, S. Kawai, M. Inoue, H. Kondo, and H. Kitasato. 2006. Induction of triggering receptor expressed on myeloid cells 1 in murine resident peritoneal macrophages by monosodium urate monohydrate crystals. *Arthritis Rheum.* 54: 455–462.
43. Shanif, M., J. G. Worrall, B. Singh, R. S. Gupta, P. M. Lydyard, C. Lambert, J. McCulloch, and G. A. Rook. 1992. The development of monoclonal antibodies to the human mitochondrial 60-kd heat-shock protein, and their use in studying the expression of the protein in rheumatoid arthritis. *Arthritis Rheum.* 35: 1427–1433.

Allergology International. 2005;54:117-122

ORIGINAL ARTICLE

Positional Effect of Amino Acid Replacement on Peptide Antigens for the Increased IFN-γ Production from CD4T Cells

Tianyi Liu[1], Hitoshi Kohsaka[2], Motoharu Suzuki[1], Rie Takagi[1], Kumiko Hashimoto[1], Yasushi Uemura[1], Hideki Ohyama[1] and Sho Matsushita[1]

ABSTRACT

Background: Based on the fact that site-specific amino acid replacement on peptide antigens stimulated T cell clones to produce increased amount of IFN-γ, we investigated this structure-function relationship, using various peptide analogues.

Methods: We used three human Th0 clones (BC20.7,BC33.5 and BC42.1) that express distinct TCRα and TCRβ chains, but recognize the same TCR ligand ; *i.e.*, the same framework of peptide antigen BCGa p84-100 in the context of DRB1*1405. These T cells were stimulated with various peptide analogues, followed by determination of proliferative responses and IFN-γ production.

Results: Replacement of Leu at peptide position 2 (P2) by amino acids which are less hydrophobic than the wild type (Val, Ala) or those with similar structural or neutral charge (Thr, Ser), induced increased IFN-γ production from T cells. This phenomenon was associated with structural features of TCR, especially the length of CDR3 region of TCRα. Amino acid replacement at the other positions did not induce increased IFN-γ production.

Conclusions: Amino acid substitution at P2 frequently induces increased IFN-γ production in a clone-specific manner, which is associated with the structure of CDR3 in TCRVα chains.

KEY WORDS

analogue peptide, complementarity determining region 3, interferon gamma, peptide antigens, T-cell antigen receptor

INTRODUCTION

Recent studies showed that T cell activation is not an all-or-none type of event ; rather, qualitative changes in T cell responses can be induced by amino acid substitutions by either MHC molecules or antigenic peptides, *i.e.*, TCR ligands. Flexibility in recognition results in T-cell activation in the absence of a proliferative response, which is designated by the following terminology as demonstrated in previous studies by our group and others : partial agonism,[1] TCR antagonism,[2] anergy,[3] survival[4] and cytokine-specific up-regulation.[5,6]

Amino acid residues on antigenic peptides have been roughly divided into two groups ; one that is important for binding to TCR (T cell epitope), and the other that is important for binding to MHC (MHC anchor). However, the crystal structure of the human class II HLA-DR1 complexed with the influenza peptide reported by Stern *et al.*[7] demonstrated that all the amino acid residues of the influenza virus peptide physically made contact with both HLA and TCR, with the exception of only one residue at the amino terminus which is buried deeply in the groove of class II, hence, there is no possibility for interaction with TCR.

[1]Department of Allergy and Immunology, Saitama Medical School, Moroyama and [2]Dapartment of Bioregulatory Medicine and Rheumatology, Graduate School, Tokyo Medical and Dental University, Tokyo, Japan.
Correspondence: Sho Matsushita, Department of Allergy and Immunology, Saitama Medical School, 38 Morohongo, Moroyama, Saitama 350-0495, Japan.
Email: shomat@saitama-med.ac.jp
Received 5 May 2004. Accepted for publication 9 April 2004.

In our previous studies, single amino acid substitutions on a group I allergen in the *Cryptomeria japonica* -derived peptide resulted in a significant increase in IFN-γ production, with no remarkable changes either in proliferative response or IL-4 production.[5] In this study, by using various analogue peptide species, we stimulated three human Th0 clones that express distinct TCRα and TCRβ chains, but recognize the same TCR ligand, and tried to determine the structure-function relationship that leads to increased IFN-γ production from T cells.

METHODS

SYNTHESIS OF PEPTIDES

The wild-type BCGa p 84-100 (EEYLILSARDVLAVVSK) and its analogue were synthesized using a solid-phase simultaneous multiple peptide synthesizer PSSM-8 (Shimadzu Corp., Kyoto, Japan), and were purified by C18 reverse-phase HPLC (Millipore).

T CELL CLONES

BCGa p84-100-specific T cell lines were established as described.[8] Three human CD4+ T cell clones (BC 20.7,BC33.5 and BC42.1) specific to BCGa p84-100+ DRA/DRB1*1405, yet bearing distinct TCRβ (BV13S3 ,BV6S1 and BV5S4, respectively ;)[8] established from PBMC of a BCG-primed healthy individual as described elsewhere,[4] were used throughout the study. T cells were fed 50 U/ml human rIL-2 and irradiated autologous PBMC prepulsed with the wild-type BCGa p84-100 on a weekly basis.

ASSESSMENT OF T-CELL RESPONSES

Antigen-induced proliferation of the T cell clones were assayed by culturing the T cells (3×10^4/well) in 96-well flat-bottomed culture plates in the presence of a peptide(s) and irradiated PBMC (1.5×10^5/well), using RPMI 1640 medium (Gibco, Grand Island, N.Y.) supplemented with 2 mM L-glutamine, 100 units/ml of penicillin, 100 μg/ml of streptomycin, and 10% heat-inactivated autologous plasma. For the proliferation assay, cells were cultured for 72 hr in the presence of 1 μCi/well of[^{3}H]thymidine during the final 16 hrs. Culture supernatants collected immediately before the addition of[^{3}H]thymidine were used to determine lymphokine concentrations, using hGM-CSF ELISA kits (R&D systems) and hIFN-γ ELISA kits (Otsuka,Tokyo,Japan).

DETERMINATION OF TCRA GENE USAGE BY T CELL CLONES

To determine TCRVA gene usage of the T cell clones that were cultured with irradiated autologous PBMC, RNA were extracted from the cell mixture, and converted to cDNA. TCRA variable region cDNA were amplified with anchored PCR as described previously for amplification of TCRA variable region cDNA.[9] A primary PCR was followed by two sequential nested PCR. TCRAC-specific primers used for primary PCR, nested PCR, and final PCR were CA4 (5'-CAG AAT CCT TAC TTT GTG AC), CA3 (5'-ATC GGT GAA TAG GCA GAC AG), and biotinylated CA5 (5'- CAC

Table 1 A panel of labeled TCRAV-specific oligonucleotide probes

AV gene	sequence	pool
AV4, 20	TGCTAAGACCACA/CCAGCC	A
AV11	TCTTCAGAGGGAGCTGTG	A
AV2	ATCCTTGAGAGTTTTACT	B
AV8a	CCATTCGAGCTGTATTTA	B
AV8b	GCATTCGAGCTTTATTTA	B
AV15	CATTTGCTGGATTTTCGT	B
AV17	GATCTTAGGAGCATCATT	B
AV21	TGGGGGCATCAGTGCTGA	B
AV3	GAGAAGAGGATCCTCAGG	C
AV5	ACTATTCTCCAGCATACT	C
AV10	CCGTGTCCATTCTTTGGA	C
AV13	GAGAGGAATACAAGTGGA	C
AV19	CAATTTTTGTTGGCTATT	C
AV24	AGCATCTGACGACCTTCT	C
AV25	TCCTTGAACATTTATTAA	C
AV26	CCTAGGGATATTGGGGTT	C
AV27	GAAAAAACTATACCATCT	C
AV29	CAGGCACCTTGTTGTGGC	C
AV32	ACTCATCACATCAATGTT	C
AV18	CTTTGGCAGCCCCATTAC	D
AV23	GAGACCCTCTTGGGCCTG	D
AV28	ACTAACTTTCGAAGCCTA	D
AV30	GGAGTGTGCATTCATAGT	D
AV7	GGAGGCACTA/GCAGGACAA	E
AV6	ACAGCTTCACTGTGGCTA	F
AV12	TGCCAGCCTGTTGAGGGC	F
AV14	GTGA/GTCTCCACCTGTCTT	F
AV1a	CTCCTGTTGCTCATACCA	G
AV1b	CTCCTGCTGCTCGTCCCA	G
AV1c	CTCCTGGAGCTTATCCCA	G
AV9	AAGCCCACCCTCATCTCA	G
AV16	GCCTCTGCACCCATCTCG	G
AV22	CTGATACTCTTACTGCTT	G
AV31	CCTCTCTGGACTTTCTAA	G

Oligomucleotide probes specific to TCRAV family genes. Degenerated probes were used to specify AV4 and AV20, AV7, and AV14 families. Three probes for AV1 family, and two probes for AV8 family were required to specify all members of each family. These probes were grouped into seven pools (pool A to G) depending on sequence similarity.

Table 2 TCRVA and TCRVB usage of BC clones

BC clone	TCRVA	TCRVB
20.7	(AV25S1)FCAGHNAG(AJ14S3)	(BV12S3)CASRQAGTAYE(BJ2S7)
33.5	(AV3S1)FCATERGQ(AJ13S2)	(BV6S1A1)CASSPTGTANT(BJ1S1)
42.1	(AV8S1A1)FCAASLDNY(AJ126)	(BV5S1A1)CASRRSTGE(BJ2S2)

TCRVA and VB usage are shown, with amino acid sequences in the N(D)N region.

TGG ATT TAG AGT CTC TC), respectively. A panel of labeled TCRAV-specific oligonucleotide probes (Table 1) were used to study TCRAV gene usage with PCR-ELISA.[10] First, seven pools of the AV-specific probes were hybridized with immobilized PCR products in microplates to find out positive wells. Then, the products were hybridized with individual AV probes in another set of plates to pin-point the AV genes predominantly used by the cDNA. To clone the entire variable region cDNA, cDNA were amplified with CA4 and reamplified with a nested primer, CA2 (5'-ACG CGT CGA CAC TGG ATT TAG AGT CTC TC). The products were subcloned into pBluscript II SK+ (Stratagene, La Jolla), and recombinant clones with the dominant VA gene were selected with dot blot DNA hybridization using corresponding VA-specific oligonucleotides. After sequence determination of these clones, dominant clones were selected as cDNA for the T cell clones.

RESULTS

TCRVA AND VB SEQUENCES

TCRVA and VB sequences of three T-cell clones BC 20.7, BC33.5 and BC42.1 are shown in Table 2. The N (D) N region sequences are shown as one-letter codes for amino acids, between V and J segments in parentheses. As described in our earlier studies, these T-cell clones recognize BCGa p84-100 (EEYLILSARDVLAVVSK; with first anchor underlined), in the context of HLA-DRB1*1405.[4] It is especially important to note that N(D)N region consists of 8 and 11 residues at TCRVA and VB of BC20.7 and BC33.5, respectively, whereas that of BC42.1 consists of 9 and 9 residues, repectively.

STIMULATORY ACTIVITIES OF BCGA P84-100-DERIVED ANALOG PEPTIDE L87V TO BC20.7

To evaluate the effects of single amino acid substitutions, proliferation and lymphokine production in response to analogue peptides were determined and findings were compared with those seen with the wild-type peptide. Most of the analogue peptides that stimulated BC clones showed a pattern of lymphokine production similar to that for the wild-type peptide (not shown). However, IFN-γ production of BC20.7 was increased in response to several analogue peptides at high concentration (16 μM), especially peptide L87V in which Leu is replaced by Val at the 87th residue of the peptide BCGa p84-100, whereas neither T cell proliferation nor production of other lymphokines, showed any remarkable change; *i.e.*, only the production of IFN-γ was affected for recognition of the analog peptide L87V. As shown in Figure 1, to determine whether or not the change of IFN-γ production was due to differences in the HLA-peptide or TCR-TCR ligand avidity between L87V and the wild-type peptide, responses of BC20.7 to several different concentrations of L87V were compared with those of the wild-type peptide. In the range of concentrations from 0.016 μM up to 16 μM, IFN-γ production in response to L87V constantly exceeded that of the wild-type peptide. Moreover, the plateau level of L87 V-driven IFN-γ production was significantly higher. Mean IFN-γ production of BC20.7 for L87V increased significantly in comparison to the wild-type, whereas no statistical differences were noted in proliferative responses between R21K and the wild-type at a range of 0.16 μM to 16 μM. The IL-4 production of BC20.7 for each analogue peptide was proportional to the proliferative response to each peptide, at a range of 0.0016 to 16 μM (not shown). In contrast, production of GM-CSF gradually increased, in a dose-dependent manner throughout the range of 0.016 to 16 μM. These data indicate that the plateau responses and proliferation of IFN-γ are not due to saturation of the TCR ligand on the APC surface.

STIMULATORY ACTIVITIES OF BCGA P84-100-DERIVED ANALOGUES TO THREE BC CLONES

All three T-cell clones were stimulated with analogues at 16 μM, with replacements at P1 (=86Y) through P9 (=94V). Table 3 summarizes the results, regarding proliferative responses and IFN-γ production. P1 (=86Y) replaced by Ala (A) indicates a peptide species EEALILSARDVLAVVSK. Relative IFN-γ responses are shown, where IFN-γ production was divided by proliferation. P1 replaced by A gave values of 96/100/98, indicating that BC20.7,BC33.5 and BC 42.1 exhibited 96%, 100% and 98% responses respectively, as compared with the wild-type. Asterisks indicate peptide species that did not exert full agonistic activity; *i.e.*, peptide stimulation even at 16 μM did not give a plateau response.

Most of analogues that exhibited full agonistic activity, stimulated IFN-γ production at levels roughly similar to the wild-type peptide, *i.e.*, at around 100%. However, it is important to note that L87T,L87S,L87A, and L87V significantly ($p<0.01$) induced increased levels of IFN-γ production of BC20.7 and BC33.5, but not of BC42.1. Such a clone-specific phenomenon was

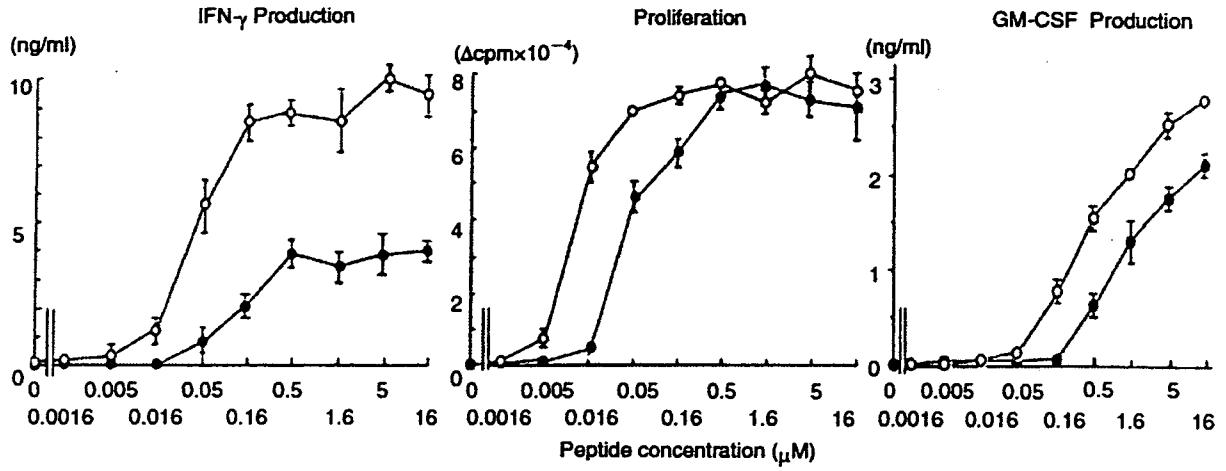

Fig. 1 IFN-γ production, GM-CSF production and proliferation of BC20.7 in recognition of either the wild-type peptide or L87V, at different concentrations. BC20.7 cells were cultured in triplicate with peptides and irradiated autologous PBMC, at the indicated concentrations. After 48-h incubation, supernatant fluids of triplicate cultures were collected. The remaining cells were pulsed with [^{3}H]-thymidine, harvested after 16h, and subjected to liquid scintillation counting. Closed circle, wild type peptide; open circle, L87V. Results are expressed as the geometric means ± standard error. IFN-γ production induced by L87V was significantly ($p<0.01$) higher than that induced by the wild-type peptide, at peptide concentrations ranging from 0.016 to 16 μM. On the other hand, plateau level of proliferation did not exhibit a significant difference, between 0.16 and 16 μM ($p>0.05$). GM-CSF production did not reach a plateau response even at 16 μM, without any statistical difference between L87V and the wild-type peptide, at 16 μM.

also observed when P5- and P8-substituted analogues were tested. Thus, S90E,S90G,S90M,D93Q,D93T and D93Y exhibited full agonism, in a clone-specific manner.

DISCUSSION

It is not very easy to identify TCR genes used by T cell clones, since they are usually cultured with irradiated autologous PBMC that includes polyclonal T cells. Random cloning of TCR cDNA derived from the cultured cells is minimally helpful in the identification, unless a large number of clones are examined. This problem was circumvented by the use of PCR-ELISA that was developed for TCRBV use,[9] and established in the present report for TCRVA usage. This technique allowed us to quantitate TCRV gene usage in the cDNA samples, and thus to identify the TCRV gene used by the T cell clones.

Three T-cell clones used in the present study recognize the same TCR ligand, as proven in our previous study. This is based on the fact that these clones recognize BCGa p84-100(^{84}EEYLILSARDVLAVVSK^{100}) in the context of DRB1*1405, and react to truncated peptides in a similar fashion.[11] Both BC20.7 and BC33.5 have 8 and 11 residues at N(D)N region of TCRVA and VB, respectively, whereas BC42.1 alone exhibits a different pattern, *i.e.*, 9 residues at N(D)N regions of TCRVA and VB. When peptide antigen is presented by class II MHC molecules, the N-terminal half of antigenic peptide is recognized mainly by CDR3 of TCRVA, whereas the C-terminal half is recoginized by CDR3 of TCRVB, which corresponds to N(D)N regions.[12] Interestingly, certain amino acid replacements on P2 induced increased IFN-γ production in BC20.7 and BC33.5 but not in BC42.1 cells, whereas those on P8 exhibited full agonism in BC 42.1 cells alone. It is thus likely that structural features of VACDR3 and VBCDR3 are responsible for specific responses induced by P2 and P8 analogues, respectively. Shuffling of N(D)N sequences between BC 42.1 and BC 20.7, or between BC 42.1 and BC 33.5 is underway to address this point.

Only L87T,L87S,L87A,and L87V induced IFN-γ enhancement. These arrangements are either smaller hydrophobic (A and V), or structurally similar neutral amino acids (T and S), indicating that close contact between P2 and TCRVA is taking place. Indeed, such a phenomenon is also seen in B-cell somatic hypermuation.[13] Thus, B-cell V region mutation in immunoglobulin heavy chain genes shows higher affinity than the germ-line sequence, usually associated with Gly, Ala, Val, Ser, Thr, or Cys, *i.e.*, small hydrophobic or small neutral residues. Apparently these mutations are not associated with static charges, but can affect either hydrogen bonding, van der Waar's force, or hydrophobic interactions.

In our previous studies using cedar pollen-derived peptides, T to V replacement on P2 also induced IFN-

Table 3 Increased IFN-γ production induced by peptide analogues

Replaced by	Relative IFN-γ response (BC20.7 / BC33.5 / BC42.1)								
	P1 =86Y	P2 =87L	P3 =88I	P4 =89L	P5 =90S	P6 =91A	P7 =92R	P8 =93D	P9 =94V
K	*/*/*	*/*/*	*/*/*	*/*/*	*/*/*	*/*/*	108/115/90	*/*/*	*/*/*
E	*/*/*	*/*/*	*/*/*	*/*/*	*/105/94	*/*/*	*/*/*	*/*/*	*/*/*
Q	*/*/*	88/79/90	*/*/*	92/79/81	*/*/*	*/*/*	*/*/*	*/*/87	*/*/*
N	*/*/*	105/97/95	*/*/*	88/92/97	*/*/*	*/*/*	*/*/*	*/*/*	*/*/*
T	*/*/*	177/210/86	110/92/81	*/*/*	77/97/108	*/*/*	*/*/*	*/*/95	85/96/91
S	*/*/*	155/187/90	95/95/99	*/*/*	100/100/100	81/87/97	*/*/*	*/*/*	93/75/99
G	*/*/*	110/98/79	90/100/92	*/*/*	*/*/115	77/69/93	*/*/*	*/*/*	94/99/100
A	96/100/98	189/202/94	105/94/83	107/93/83	88/104/110	100/100/100	*/*/*	*/*/*	80/81/92
V	91/91/85	271/259/92	91/84/86	105/96/86	99/100/101	90/76/85	*/*/*	*/*/*	100/100/100
L	93/88/102	100/100/100	100/90/101	100/100/100	*/*/*	*/*/*	*/*/*	*/*/*	*/*/*
Y	100/100/100	*/*/*	*/*/*	*/*/*	*/*/*	*/*/*	*/*/*	*/*/98	*/*/*
M	89/93/91	*/*/*	96/99/103	89/70/85	*/91/*	*/*/*	*/*/*	*/*/*	*/*/*
W	90/103/109	*/*/*	*/*/*	*/*/*	*/*/*	*/*/*	*/*/*	*/*/*	*/*/*

Positions 1 - 9 (P1 - P9) of BCGa p84-100 (EEYLILSARDVLAVVSK, with P1 underlined), was replaced by indicated amino acids. T cells were stimulated with peptide species at 16 μM. To obtain relative IFN-γ response values, plateau responses of IFN-γ (pg/ml) were first divided by plateau responses of proliferation (cpm). Then, the following calculation was performed; relative IFN-γ responses=100x[IFN-γ/proliferation to analogues]/[IFN-γ/proliferation to the wild-type BCGa p84-100]. The denominator was 0.0533. *Peptide that did not induce fully agonistic proliferation.

γ enhancement, whereas proliferation remained the same. Therefore, although not generalized, mutual replacement on G, A, V, L, S, or T at P2, tends to induce IFN-γ-specific enhancement. Such observations also have been reported in another study with different peptide species.[14] In this sense, analogue-induced clonal anergy is often observed, especially when residue replacement is made on P7 or P8.[11] Moreover, truncation of the C-terminal moiety of antigenic peptides, in general, exhibit TCR antagonism.[15] In other words, if a rule that applies to altered polyclonal novel responses induced by peptide analogues is established, it will lead us to novel therapeutic interventions using peptide analogues. Our observations on P2 replacement which is associated with increased IFN-γ production are imperative to furthering our understanding.

ACKNOWLEDGEMENTS

This work was supported by the Ministry of Health, Labour and Welfare, Japan.

REFERENCES

1. Evavold BD, Allen PM. Separation of IL-4 production from Th cell proliferation by an altered T cell receptor ligand. *Science* 1991;252:1308.
2. Chen Y-Z, Matsushita S, Nishimura Y. Response of a human T cell clone to a large panel of altered peptide ligands carrying single residue substitutions in an antigenic peptide : characterization and frequencies of TCR agonism and TCR antagonism with or without partial activation. *J. Immunol.* 1996;13:3783-3790.
3. Sloan-Lancaster J, Evavold BD, Allen PM. Induction of T-cell anergy by altered T-cell-recepter ligand on live antigen-presenting cells. *Nature* 1993;363:156.
4. Matsushita S, Kohsaka H, Nishimura Y. Evidence for self- and non-self- peptide partial agonists that prolong clonal survival of mature T cells in vitro. *J. Immunol.* 1997;158: 5685-5691.
5. Ikagawa S, Matsushita S, Chen Y-Z, Ishikawa T, Nishimura Y. Single amino acid substitutions on a Japanese cedar pollen allergen (Cry j I)- derived peptide induced qualitative changes in human T cell responses and T cell receptor antagonism. *J. Allergy Clin. Immunol.* 1996;97:53-67.
6. Windhagen A, Scholz C, Höllsberg P, Fukaura H, Sette A, Hafler DA. Modulation of cytokine patterns of human autoreactive T cell clones by a single amino acid substitution of their peptide ligand. *Immunity* 1995;2:373.
7. Stern LJ, Brown JH, Jardetzky TS *et al.* Crystal structure of the human class II MHC protein HLA-DR1 complexed with an influenza virus peptide. *Nature* 1994;368:215-221.
8. Matsushita S, Yokomizo H, Kohsaka H, Nishimura Y. Diversity of a human $CD4^+$ T cell repertoire recognizing one TCR ligand. *Immunol. Lett.* 1996;51:191.
9. Kohsaka H, Taniguchi A, Chen PP, Ollier WER, Carson DA. The expressed T cell receptor V gene repertoire of rheumatoid arthritis monozygotic twins : rapid analysis by anchored polymerase chain reaction and enzyme-linked immunosorbent assay. *Eur. J. Immunol.* 1993;23: 1895-1901.
10. Nanki T, Kohsaka H, Mizushima N, Carson DA, Miyasaka N. Genetic control of human TCRBJ gene repertoires of peripheral T lymphocytes of normal and rheuma-

toid arthritis monozygotic twins. *J. Clin. Invest.* 1996;98: 1594-1601.

11. Matsushita S, Nishimura Y. Partial activation of human T cells by peptide analogs on live APC : induction of clonal anergy associated with protein tyrosine dephosphorylation. *Hum. Immunol.* 1997;53:73-80.
12. Hennecke J, Carfi A, Wiley DC. Structure of a covalently stabilized complex of a human αβ T-cell receptor, influenza HA peptide and MHC class II molecule, HLA-DR1. *EMBO J.* 2000;19:5611-5624.
13. Rogozin IB, Kolchanov NA. Somatic hypermutagenesis in immunoglobulin genes. II. Influence of neighbouring base sequences on mutagenesis. *Biochem. Biophys. Acta.* 1992;1171:11.
14. Yssel H, Johnson KE, Schneider PV. T cell activation-inducing epitope on the house dust mite allergen Der p 1. Proliferation and lymphokine production patterns by Der p 1-specific CD4+ T cell clones. *J. Immunol.* 1992;148: 738-745.
15. Matsushita S, Matsuoka T. Peptide length-dependent TCR antagonism on class II HLA-restricted responses of PBMC and T-cell clones. *Eur. J. Immunol.* 1999;29:431-436.

Inhibition of CX3CL1 (Fractalkine) Improves Experimental Autoimmune Myositis in SJL/J Mice[1]

Fumihito Suzuki,* Toshihiro Nanki,[2]* Toshio Imai,[†] Hirotoshi Kikuchi,[‡] Shunsei Hirohata,[‡] Hitoshi Kohsaka,* and Nobuyuki Miyasaka*

Idiopathic inflammatory myopathy is a chronic inflammatory muscle disease characterized by mononuclear cell infiltration in the skeletal muscle. The infiltrated inflammatory cells express various cytokines and cytotoxic molecules. Chemokines are thought to contribute to the inflammatory cell migration into the muscle. We induced experimental autoimmune myositis (EAM) in SJL/J mice by immunization with rabbit myosin and CFA. In the affected muscles of EAM mice, CX3CL1 (fractalkine) was expressed on the infiltrated mononuclear cells and endothelial cells, and its corresponding receptor, CX3CR1, was expressed on the infiltrated CD4 and CD8 T cells and macrophages. Treatment of EAM mice with anti-CX3CL1 mAb significantly reduced the histopathological myositis score, the number of necrotic muscle fibers, and infiltration of CD4 and CD8 T cells and macrophages. Furthermore, treatment with anti-CX3CL1 mAb down-regulated the mRNA expression of TNF-α, IFN-γ, and perforin in the muscles. Our results suggest that CX3CL1-CX3CR1 interaction plays an important role in inflammatory cell migration into the muscle tissue of EAM mice. The results also point to the potential therapeutic usefulness of CX3CL1 inhibition and/or blockade of CX3CL1-CX3CR1 interaction in idiopathic inflammatory myopathy. ***The Journal of Immunology,*** **2005, 175: 6987–6996.**

Idiopathic inflammatory myopathy (IIM),[3] including polymyositis and dermatomyositis, is characterized by chronic inflammation of the voluntary muscles associated with infiltration of inflammatory cells, including CD4 and CD8 T cells and macrophages, in the skeletal muscle (1–3). Infiltrated CD4 and CD8 T cells express cytotoxic molecules, such as perforin and granzyme granules, and the T cells and macrophages express inflammatory cytokines, such as TNF-α and IFN-γ (4–8). Therefore, the infiltrated inflammatory cells might play an important role in the pathogenesis of IIM. The inflammatory cell migration into the muscle is thought to involve the interaction of chemokines and chemokine receptors (9–14).

Chemokines are involved in leukocyte recruitment and activation at the site of inflammatory lesion (15). Approximately 50 chemokines have been identified to date, and they are classified into four subfamilies, C, CC, CXC, and CX3C chemokines, based on the conserved cystein motifs (16). Although the majority of chemokines are small secreted molecules, CX3CL1 (fractalkine) is expressed on the cell surface as a membrane-bound molecule (17, 18). The membrane-bound CX3CL1 is expressed on endothelial cells stimulated with TNF-α, IL-1, and IFN-γ (19–21), induces adhesion of the leukocytes, and supports leukocyte transmigration into tissue (22, 23). The soluble form of CX3CL1 is generated by proteolytic cleavage at a membrane-proximal region of the membrane-bound CX3CL1 by TNF-α-converting enzyme (a disintegrin and metalloproteinase domain 17) and a disintegrin and metalloproteinase domain 10 (24, 25), and is known to induce leukocyte migration (23). In contrast, CX3CR1, a unique receptor for CX3CL1, is expressed on peripheral blood CD4 and CD8 T cells that express cytotoxic molecules and type 1 cytokines (26, 27). CX3CR1 is also expressed on monocytes/macrophages, NK cells, and dendritic cells (28, 29).

Based on the infiltration of CTLs and macrophages into the affected muscles in patients with IIM, we speculated that the CX3CL1-CX3CR1 interaction might contribute to the inflammatory cell migration. In the present study we induced experimental autoimmune myositis (EAM) in SJL/J mice and examined CX3CL1 and CX3CR1 expression in the affected muscle of EAM mice. Furthermore, we studied the effect of CX3CL1 inhibition on EAM mice.

Materials and Methods

Induction of EAM

Male 5-wk-old SJL/J mice were purchased from Charles River Japan. Purified myosin from rabbit skeletal muscle (6.6 mg/ml; Sigma-Aldrich) was emulsified with an equal amount of CFA (Difco Laboratories) with 3.3 mg/ml *Mycobacterium butyricum* (Difco Laboratories). Mice were immunized intracutaneously with 100 μl of emulsion into four locations (total, 400 μl) on the back on days 0, 7, and 14. On day 21, the mice were killed, and the quadriceps femoris muscles were harvested. The muscle tissues were frozen immediately in chilled isopentane precooled in liquid nitrogen, and then 6-μm-thick cryostat sections were prepared at intervals of 200 μm. The sections were stained with H&E or used for immunohistochemistry. The experimental protocol was approved by the institutional animal care and use committee of Tokyo Medical and Dental University.

Immunohistochemistry

Immunohistological staining was performed as described previously (26, 30) with some modifications. Briefly, 6-μm-thick sections were air-dried and fixed in cold acetone at −20°C for 3 min. After air-drying at room

*Department of Medicine and Rheumatology, Tokyo Medical and Dental University Graduate School, Tokyo, Japan; [†]KAN Research Institute, Kyoto, Japan; and [‡]Department of Internal Medicine, Teikyo University School of Medicine, Tokyo, Japan

Received for publication January 4, 2005. Accepted for publication September 1, 2005.

The costs of publication of this article were defrayed in part by the payment of page charges. This article must therefore be hereby marked *advertisement* in accordance with 18 U.S.C. Section 1734 solely to indicate this fact.

[1] This work was supported in part by a grant-in-aid from the Japan Intractable Diseases Research Foundation; the Fund for Intractable Diseases Research by Atsuko Ouchi from Tokyo Medical and Dental University; the Ministry of Health, Labor, and Welfare; and the Ministry of Education, Science, Sports, and Culture, Japan.

[2] Address correspondence and reprint requests to Dr. Toshihiro Nanki, Department of Medicine and Rheumatology, Tokyo Medical and Dental University Graduate School, 1-5-45, Yushima, Bunkyo-ku, Tokyo 113-8519, Japan. E-mail address: nanki.rheu@tmd.ac.jp

[3] Abbreviations used in this paper: IIM, idiopathic inflammatory myopathy; EAM, experimental autoimmune myositis; PTX, pertussis toxin.

0022-1767/05/$02.00

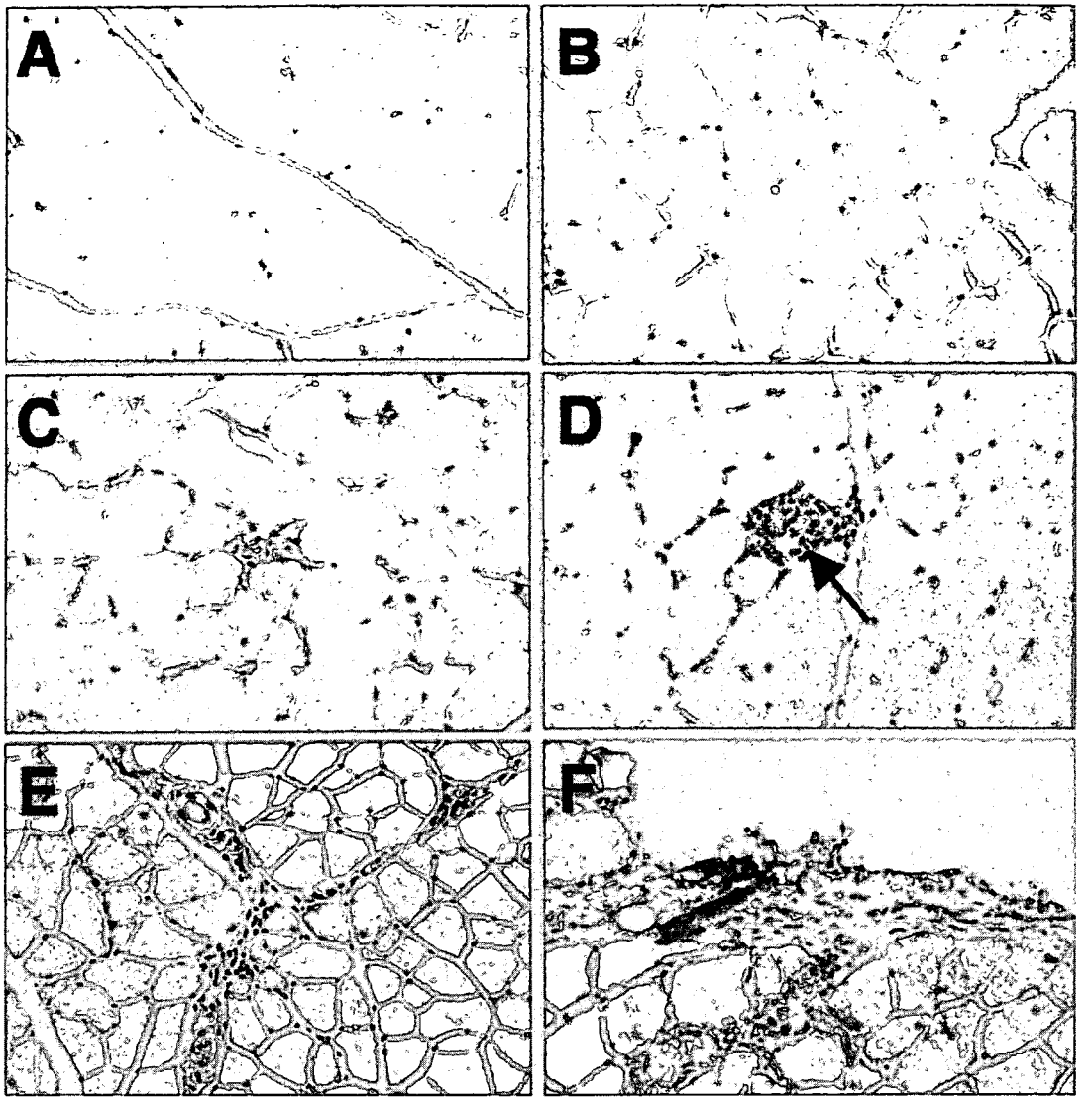

FIGURE 1. Histological changes found in the muscle of murine EAM. Quadriceps femoris muscle of normal mice and immunized mice on day 7 showed no inflammatory changes (*A* and *B*, respectively). On day 14, mild cellular infiltration in the muscle tissue was shown (*C*). Muscle tissues of EAM mice on day 21 showed cellular infiltration in the endomysium (*D*), perimysium (*E*), epimysium (*F*), and necrotic muscle fibers (arrow in *D*). H&E staining was used. Original magnification, ×200.

temperature, the slides were rehydrated in PBS for 2 min three times, and then the endogenous peroxidase activity was blocked by incubation in 1.0% H_2O_2 in PBS for 10 min, followed by rinsing for 2 min three times in PBS. Nonspecific binding was blocked with 10% normal rabbit serum in PBS for 30 min. For CD4, CD8, and F4/80 staining, the sections were incubated with 5 μg/ml rat anti-mouse CD4 mAb (GK1.5; Cymbus Biotechnology), 2 μg/ml rat anti-mouse CD8a mAb (53-6.7; BD Pharmingen), 5 μg/ml rat anti-mouse F4/80 mAb (C1:A3-1; Serotec), or normal rat IgG in Ab diluent (BD Pharmingen) overnight at 4°C. The samples were then washed three times in PBS for 5 min each time and incubated with biotin-conjugated rabbit anti-rat IgG (DakoCytomation) for 30 min at room temperature with 5% normal mouse serum. To analyze a time course of cell infiltration, numbers of $CD4^+$, $CD8^+$, and $F4/80^+$ cells in six randomly selected fields at ×200 were counted from three EAM mice on days 0, 7, 14, and 21.

For mouse vascular endothelial cell staining, we used a tyramide signal amplification kit (NEL700A; PerkinElmer). After blocking with 10% normal rabbit serum, the sections were incubated with 5 μg/ml rat anti-mouse vascular endothelial cadherin Ab (11D4.1; BD Pharmingen) or normal rat IgG overnight at 4°C. The samples were then washed three times in PBS for 5 min each time and incubated with biotin-conjugated rabbit anti-rat IgG for 30 min at room temperature with 5% normal mouse serum. After washing three times in PBS for 5 min each time, the sections were incubated with streptavidin-HRP for 30 min at room temperature and washed in PBS three times for 5 min each time. The samples were incubated with biotinyl tyramide amplification reagent at room temperature for 5 min, then washed three times in PBS for 5 min each time, and incubated again with streptavidin-HRP for 30 min. After washing three times in PBS for 5 min each time, diaminobenzidine tablets (Sigma-Aldrich) were used for visualization. The sections were counterstained in hematoxylin for 30 s and washed in tap water for 5 min.

For mouse CX3CL1 staining, the endogenous peroxidase activity was blocked by incubation in 1.0% H_2O_2 in methanol, and then the sections were incubated overnight at 4°C with goat anti-mouse CX3CL1 Ab (sc-7227; Santa Cruz Biotechnology) or normal goat IgG in Ab diluent at 5 μg/ml. The samples were then washed three times in PBS for 5 min each time and incubated with biotin-conjugated rabbit anti-goat IgG (DakoCytomation) for 30 min at room temperature with 5% normal mouse serum. After washing three times in PBS for 5 min each time, the sections were incubated with peroxidase-conjugated streptavidin (DakoCytomation) for 30 min at room temperature and washed three times for 5 min each time. For enhancing the expression of CX3CL1 on endothelial cells, a tyramide signal amplification kit was

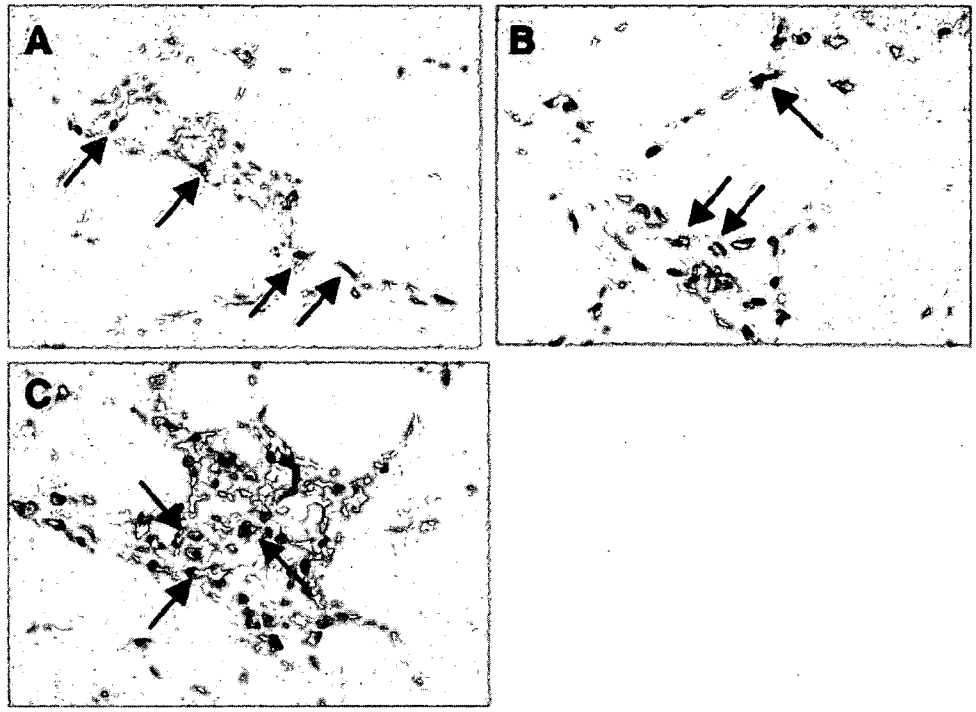

FIGURE 2. Infiltration of CD4 and CD8 T cells and macrophages in the muscles of EAM mice. Frozen sections of the quadriceps femoris muscle of EAM mice on day 21 were examined by immunohistochemistry using mAb against CD4 (*A*), CD8 (*B*), and F4/80 (*C*). The arrows indicate $CD4^+$, $CD8^+$, and $F4/80^+$ cells. Original magnification, ×200.

used as described above. Diaminobenzidine tablets were used for visualization. The sections were counterstained in hematoxylin for 30 s and washed in tap water for 5 min.

For CD4, CD8 or F4/80, and CX3CR1 double staining, the sections were incubated overnight at 4°C with 5 μg/ml rat anti-mouse CD4 mAb (GK1.5), 5 μg/ml rat anti-mouse CD8 mAb (53-6.7), 5 μg/ml rat anti-mouse F4/80 mAb (C1:A3-1), or normal rat IgG in Ab diluent. Subsequently, the samples were washed three times for 5 min each time in PBS and incubated with Alexa Fluor 488-conjugated goat anti-rat IgG (Molecular Probes) at 5 μg/ml for 1 h at room temperature. For CX3CR1 staining, the sections were washed three times in PBS for 5 min each time and then incubated with rabbit anti-mouse CX3CR1 Ab (30) or normal rabbit IgG at 5 μg/ml in Ab diluent for 2 h at room temperature. Next, the samples were washed three times for 5 min each time in PBS and incubated with Alexa Fluor 568-conjugated goat anti-rabbit IgG (Molecular Probes) at 5 μg/ml for 1 h at room temperature. The slides were examined using fluorescent microscopy (BZ-Analyzer; Keyence).

Treatment with anti-mouse CX3CL1 mAb

A mAb against murine CX3CL1 was generated from Armenian hamsters immunized with recombinant murine CX3CL1 by a standard method. One mAb, 5H8-4, was selected for additional studies. The specificity was examined by ELISA using a panel of murine CXC (MIP-2, keratinocyte-derived chemokine, and CXCL9, 10, 12, and 13), CC (CCL1–7, 9–12, 17, 19–22, 25, 27, and 28), C (XCL1), and CX3C (CX3CL1) chemokines. The mAb reacted specifically with murine CX3CL1. Five hundred micrograms of hamster anti-mouse CX3CL1 mAb (5H8-4) or control Ab (hamster IgG; ICN Pharmaceuticals) was injected into the mouse peritoneal cavity three times per week from day 0 for 3 wk. The injection of anti-CX3CL1 mAb did not affect the number of PBMC (data not shown).

The severity of inflammatory changes was classified using five grades according to the classification of Kojima et al. (31) with some modification: score 0, no inflammation; score 1, mild endomysial inflammatory changes; score 2, severe endomysial inflammatory changes; score 3, perimysial inflammatory changes in addition to score 2; and score 4, diffuse extensive lesion. If multiple lesions were found in one muscle specimen, 0.5 point was added to the indicated score. To evaluate the severity of inflammation using a different aspect, we counted the number of necrotic muscle fibers, and $CD4^+$, $CD8^+$, and $F4/80^+$ cells in continuous three sections. Each section examined six random fields at ×400. The evaluation of histopathological inflammatory changes was performed in a blind fashion for the experimental group identity.

Real-time RT-PCR

Total RNA was prepared from a 100 mg muscle block using RNA extraction solution, Isogen (Nippon Gene), and treated with DNase I (Invitrogen Life Technologies). The first-strand cDNA was synthesized using oligo$(dT)_{12-18}$ primers (Pharmacia Biotech) and SuperScript II reverse transcriptase (Invitrogen Life Technologies).

The relative quantitative real-time PCR was performed using SYBR Green I on ABI PRISM 7000 (Applied Biosystems) according to the instructions provided by the manufacturer. The cDNA was amplified with primers for TNF-α (5′, GTA CCT TGT CTA CTC CCA GGT TCT CT; 3′, GTG TGG GTG AGG AGC ACG TA), IFN-γ (5′, CCT GCG GCC TAG CTC TGA; 3′, CCA TGA GGA AGA GCT GCA AAG), perforin (5′, CCA CGG CAG GGT GAA ATT C; 3′, GGC AGG TCC CTC CAG TGA), and GAPDH (5′, ATG CAT CCT GCA CCA CCA A; 3′, GTC ATG AGC CCT TCC ACA ATG). These primers were designed using the ABI Primer Express Software program (Applied Biosystems). The reaction buffer contained the following components: 25 μl of SYBR Green PCR Master Mix (Applied Biosystems), 300 nM forward and reverse primers, 50 ng cDNA template, and RNA-free distilled water up to 50 μl of total volume. The PCR was conducted using the following parameters: 50°C for 2 min, 95°C for 10 min, and 40 cycles of denaturation at 95°C for 15 s and annealing/extension at 60°C for 1 min. GAPDH mRNA was used as an internal control to standardize the amount of sample mRNA. A validation experiment demonstrated approximately equal efficiencies of the target and reference. Thus, the relative expression of real-time PCR products was determined using the ΔΔCt method that compares the mRNA expression levels of the target gene and the housekeeping gene (32, 33). One of the control samples was chosen as a calibrator sample.

Statistical analysis

Differences in the score of tissue inflammation, number of necrotic muscle fibers, number of migrated cells, and relative expression levels of TNF-α, IFN-γ, and perforin between control Ab- and anti-mouse CX3CL1 mAb-treated EAM mice, and the relative expression levels of TNF-α, IFN-γ, and perforin between normal and EAM mice were examined for statistical significance using Mann-Whitney's *U* test. All data were expressed as the

mean ± SEM. The difference between two groups of mice was considered significant at $p < 0.05$.

Results

Development of EAM

SJL/J mice were immunized with purified rabbit myosin fraction and CFA on days 0, 7, and 14. On days 0, 7, 14, and 21, the quadriceps femoris muscles of these mice were histologically examined with H&E staining. All muscle specimens of normal SJL/J mice and immunized mice on day 7 showed normal appearance with no inflammatory changes (Fig. 1, *A* and *B*, respectively), whereas those of mice immunized with rabbit myosin fraction showed mild mononuclear cell infiltration at day 14 (Fig. 1*C*). On day 21, a significant number of mononuclear cells were infiltrated among the muscle fibers (endomysium; Fig. 1*D*), at perivascular areas (perimysium; Fig. 1*E*), and epimysium (Fig. 1*F*). Scattered lesions with aggregates of infiltrated mononuclear cells were formed, in which atrophic or necrotic muscle fibers were noted (arrow in Fig. 1*D*). Injection of PBS and CFA into SJL/J mice did not show infiltration of inflammatory cells in the quadriceps femoris muscles (data not shown).

To determine the subsets of infiltrating mononuclear cells in the quadriceps femoris muscles of EAM mice, we performed immunohistochemical analysis using mAbs against CD4, CD8, and F4/80. $CD4^+$ T cells were mainly located in the perimysium and some were found in the endomysium (Fig. 2*A*). $CD8^+$ T cells were predominantly detected in the endomysium and surrounded nonnecrotic muscle fibers (Fig. 2*B*). $F4/80^+$ macrophages were located in the endomysium as well and were especially present around the necrotic muscle fibers (Fig. 2*C*). Because these histological findings of inflammatory cell infiltration patterns resembled those of affected muscle lesions in IIM patients (34–36), we decided to use the EAM mice as an experimental model of IIM.

To evaluate a time course of cellular infiltration into the muscles, we counted the numbers of infiltrated $CD4^+$, $CD8^+$, and $F4/80^+$ cells on days 0, 7, 14, and 21 by immunohistochemical method. The majority of the infiltrating cells on day 14 were $F4/80^+$ macrophage (Fig. 3). In contrast, the number of $CD4^+$ and $CD8^+$ T cells was not increased until day 14, and they had significantly migrated into the muscles on day 21. These results were similar to previously reported data (37).

CX3CL1 and CX3CR1 expression in the muscle of EAM mice

We examined the expression of CX3CL1 in the muscle of normal SJL/J mice and EAM mice by immunohistochemistry. In the quadriceps femoris muscles of normal mice, no CX3CL1 expression was detected (Fig. 4, *A* and *G*). In contrast, CX3CL1 was expressed on infiltrated mononuclear cells predominantly in the endomysium and vascular endothelial cells of EAM mice on day 14 (Fig. 4, *B* and *H*, respectively) and day 21 (Fig. 4, *C* and *I*, respectively).

We next examined the expression of CX3CR1 on the infiltrated mononuclear cells in the quadriceps femoris muscle of EAM mice by double immunohistochemical staining. Some $CD4^+$ T cells expressed CX3CR1 (Fig. 5, *A–C*). The majority of $CD8^+$ T cells and most of the $F4/80^+$ macrophages expressed CX3CR1 (Fig. 5, *D–F* and *G–I*, respectively).

Effect of anti-mouse CX3CL1 mAb on EAM mice

To analyze the effect of anti-CX3CL1 mAb administration on EAM mice, we evaluated the histological changes in quadriceps femoris muscle using H&E staining. The incidence of inflammatory cell infiltration in control Ab-treated mice was 100% ($n = 10$). Treatment with anti-CX3CL1 mAb did not change the incidence of cellular infiltration (100%; $n = 10$). EAM mice treated with control Ab showed mononuclear cell infiltration with atrophy and necrosis of muscle fibers (Fig. 6*A*). In comparison, anti-CX3CL1 mAb-treated EAM mice showed milder histological changes (Fig. 6*B*). Analysis of histological scores of inflammatory changes in the quadriceps femoris muscles indicated that treatment with anti-CX3CL1 mAb significantly reduced inflammatory cell infiltration in the muscles of EAM mice compared with treatment with control Ab (Fig. 6*C*). Moreover, anti-CX3CL1 mAb treatment reduced the number of necrotic muscle fibers in muscles (Fig. 6*D*). A similar result was obtained in another independent set of experiments.

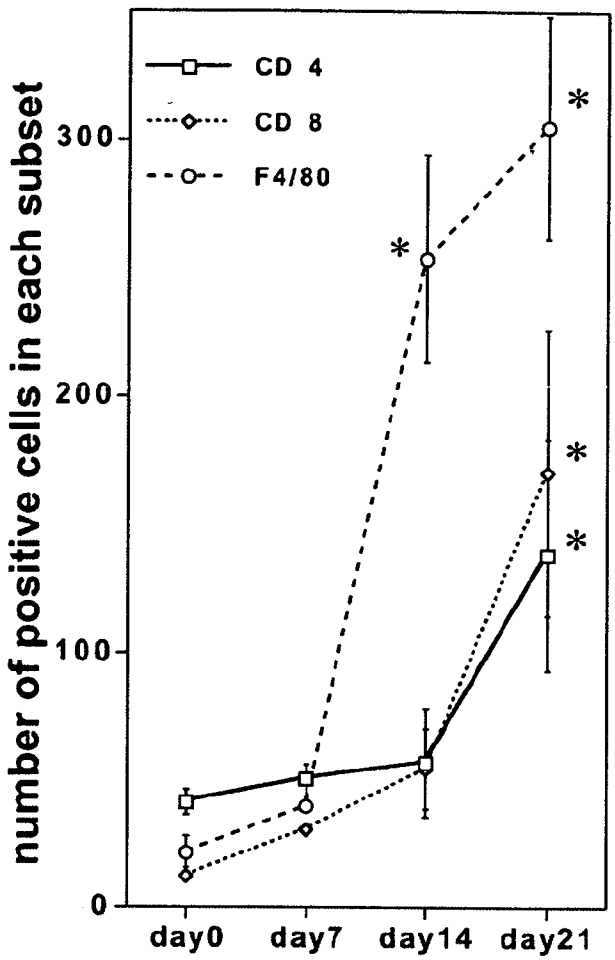

FIGURE 3. Time course of inflammatory cell infiltration into the muscle tissue of EAM mice. The numbers of infiltrating $CD4^+$, $CD8^+$, and $F4/80^+$ cells into the quadriceps femoris muscles were counted by immunohistochemistry. Data represent the mean ± SEM. *, $p < 0.05$.

We next examined the effect of anti-CX3CL1 mAb treatment on the numbers of each subset of infiltrating cells. The numbers of $CD4^+$, $CD8^+$, and $F4/80^+$ cells in quadriceps femoris muscles were counted and compared between mice treated with control Ab and those with anti-CX3CL1 mAb. Anti-CX3CL1 mAb treatment significantly reduced the number of infiltrated $CD4^+$ T cells by ~30% (Fig. 7*A*), $CD8^+$ T cells by ~50%, and $F4/80^+$ macrophages by up to 50% (Fig. 7, *B* and *C*).

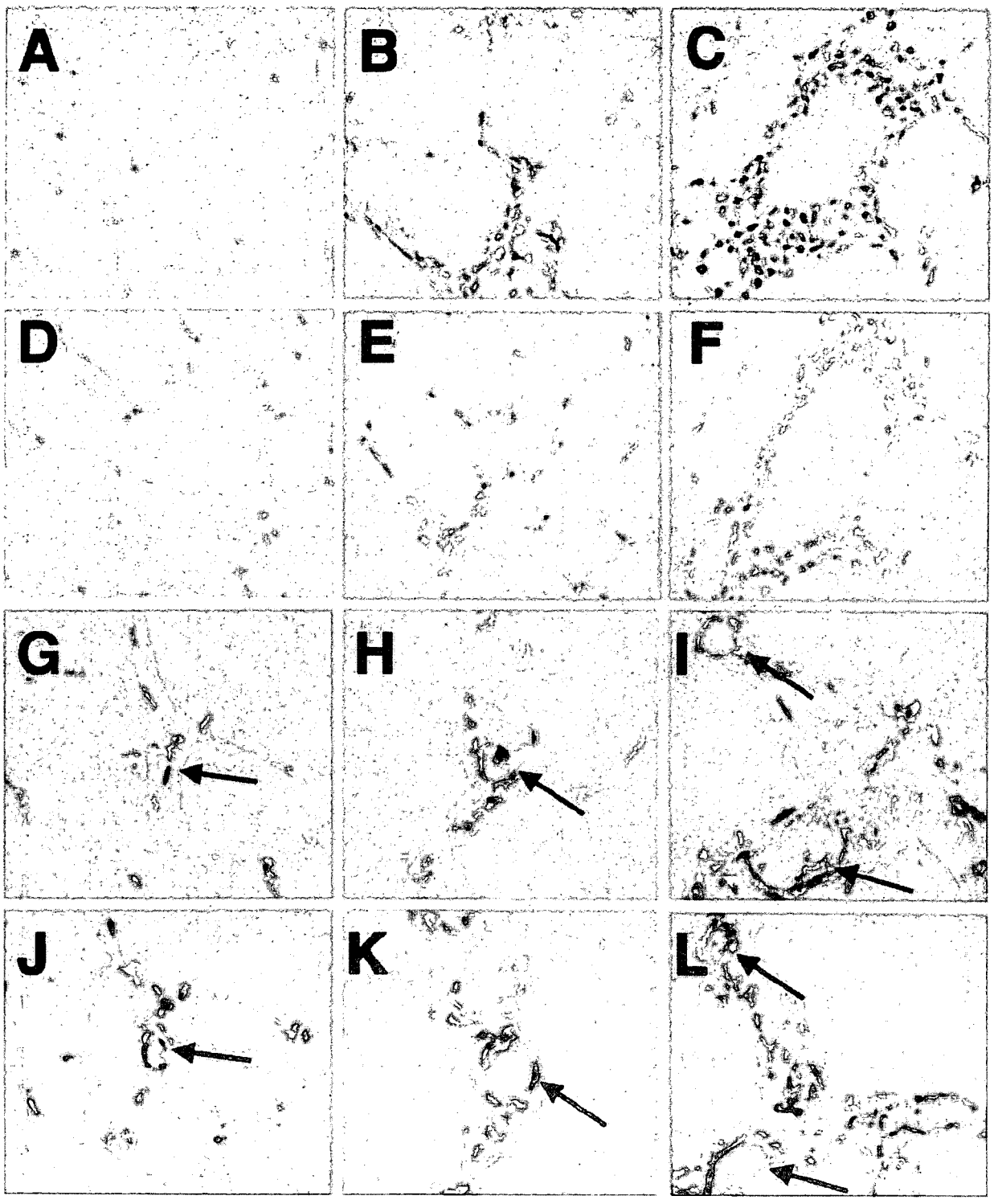

FIGURE 4. CX3CL1 expression in the muscles of EAM mice. Expression of CX3CL1 was examined by immunohistochemistry in normal mice (*A* and *G*) and EAM mice on day 14 (*B* and *H*) and day 21 (*C* and *I*). Vascular endothelial cadherin expression in the normal mice (*J*) and EAM mice on day 14 (*K*) and 21 (*L*) was also examined using serial sections with *G*, *H*, and *I*, respectively. Stainings with isotype control Ab for CX3CL1 are shown (*D*, normal mice; *E*, EAM on day 14; *F*, EAM on day 21). Arrows indicate vascular endothelial cadherin-positive endothelial cells (*J–L*), and corresponding endothelial cells (*G–I*). Original magnification, ×400.

We finally examined the effects of anti-CX3CL1 mAb treatment on the expression of cytokines and cytotoxic molecule in the quadriceps femoris muscle of EAM mice by quantitative RT-PCR. Although the relative quantities of TNF-α, IFN-γ, and perforin mRNA were very low in normal SJL/J mice, they were significantly up-regulated in EAM mice that received control Ab treatment ($p < 0.05$). Furthermore, treatment with anti-CX3CL1 mAb strikingly reduced mRNA expression (Fig. 8).

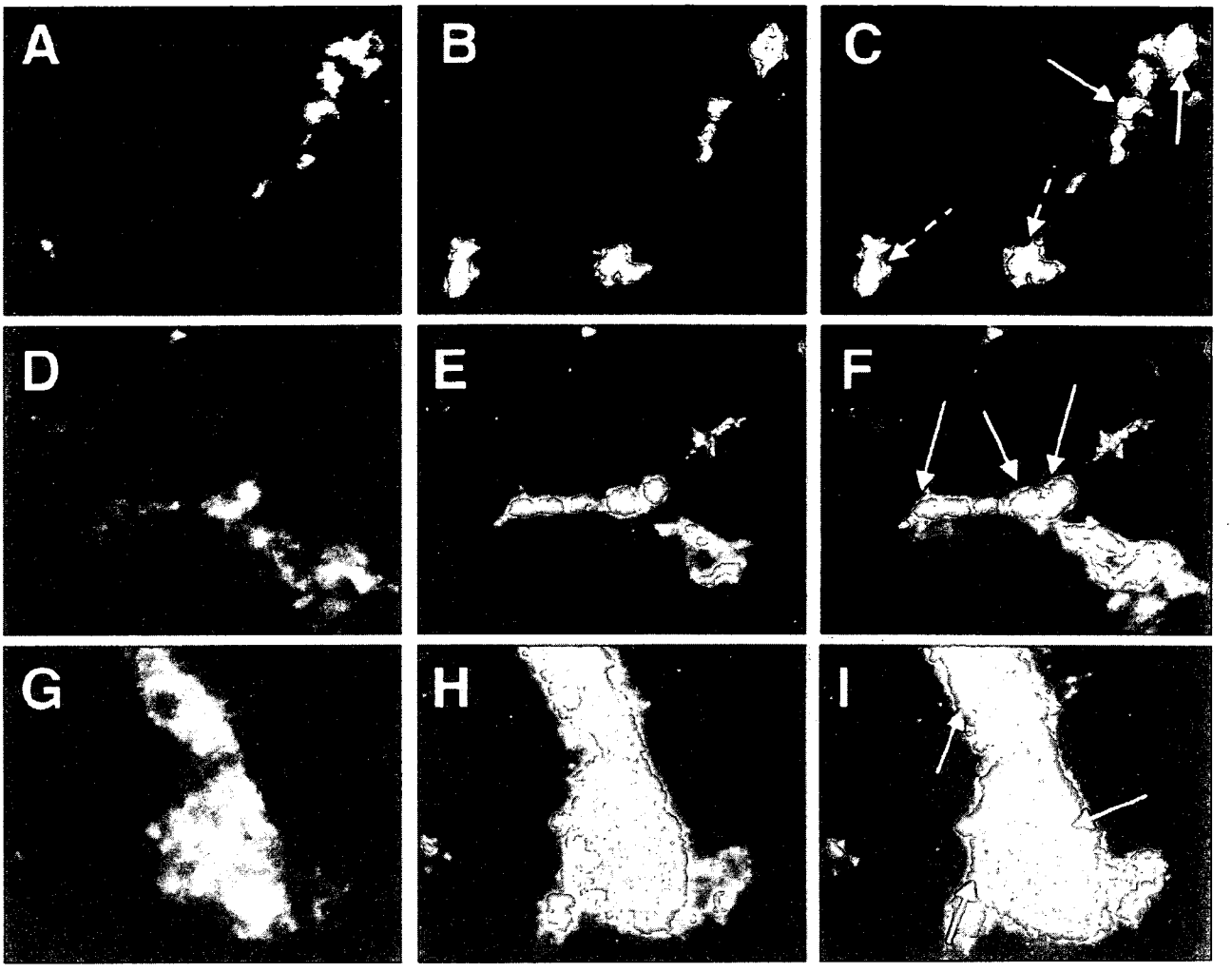

FIGURE 5. CX3CR1 expression on $CD4^+$, $CD8^+$, or $F4/80^+$ cells in the EAM muscle. Muscle tissues from EAM mice were double stained with CD4, CD8, or F4/80, and CX3CR1, and analyzed with fluorescent microscopy (*A*, CX3CR1; *B*, CD4; *C*, merged *A* and *B*; *D*, CX3CR1; *E*, CD8; *F*, merged *D* and *E*; *G*, CX3CR1; *H*, F4/80; *I*, merged *G* and *H*). Solid arrows indicate double-positive cells. Dotted arrows indicate CX3CR1-negative CD4 T cells. Original magnification, ×200.

Considered together, the above results indicate that treatment with anti-CX3CL1 mAb reduced infiltration of CD4 and CD8 T cells and macrophages and reduced the expression of various inflammatory cytokines and cytotoxic molecule in muscles.

Discussion

The major findings of the present study were the following. 1) CX3CL1 was expressed on infiltrated mononuclear cells and vascular endothelial cells, and its corresponding receptor, CX3CR1, was expressed on infiltrated inflammatory cells in the muscles of EAM. 2) Treatment with anti-CX3CL1 mAb ameliorated histological inflammatory changes in EAM mice, reduced the numbers of infiltrated CD4 and CD8 T cells and macrophages, and reduced the expression of TNF-α, IFN-γ, and perforin in the muscles. These results suggest that CX3CL1-CX3CR1 interaction seems to play an important role in inflammatory cell migration into the muscles of EAM mice.

Development of EAM in SJL/J mice by immunization with rabbit purified skeletal myosin fraction and CFA was previously reported (37–40). We modified the method by increasing the amount of immunized myosin and CFA and the addition of *Mycobacterium butyricum*. This modification shortened the period required for the development of myositis from 5 wk, which was thought to be appropriate for the induction (38), to 3 wk. Moreover, although pertussis toxin (PTX) injection into the peritoneal cavity increased the severity of inflammatory changes in the muscle (31), and thus, PTX was administered in the previous models (31, 36, 38), our modified method induces significant myositis without PTX injection. The EAM mice showed inflammatory cell infiltration in the endomysium, perimysium, and epimysium with muscle fiber necrosis. Immunohistochemical analysis showed that the invading cells surrounding nonnecrotic muscle fibers in the endomysium were mainly CD8 T cells, whereas macrophages were predominantly detected in necrotic fibers, and CD4 T cells were located in perimysium. Moreover, quantitative RT-PCR showed up-regulation of expression of TNF-α, IFN-γ, and perforin mRNA in the muscle of EAM mice. These findings in EAM mice are similar to those reported in IIM patients (4–8, 34–36).

Inflammatory cell migration into the affected muscle of IIM is thought to involve chemokine-chemokine receptor interaction

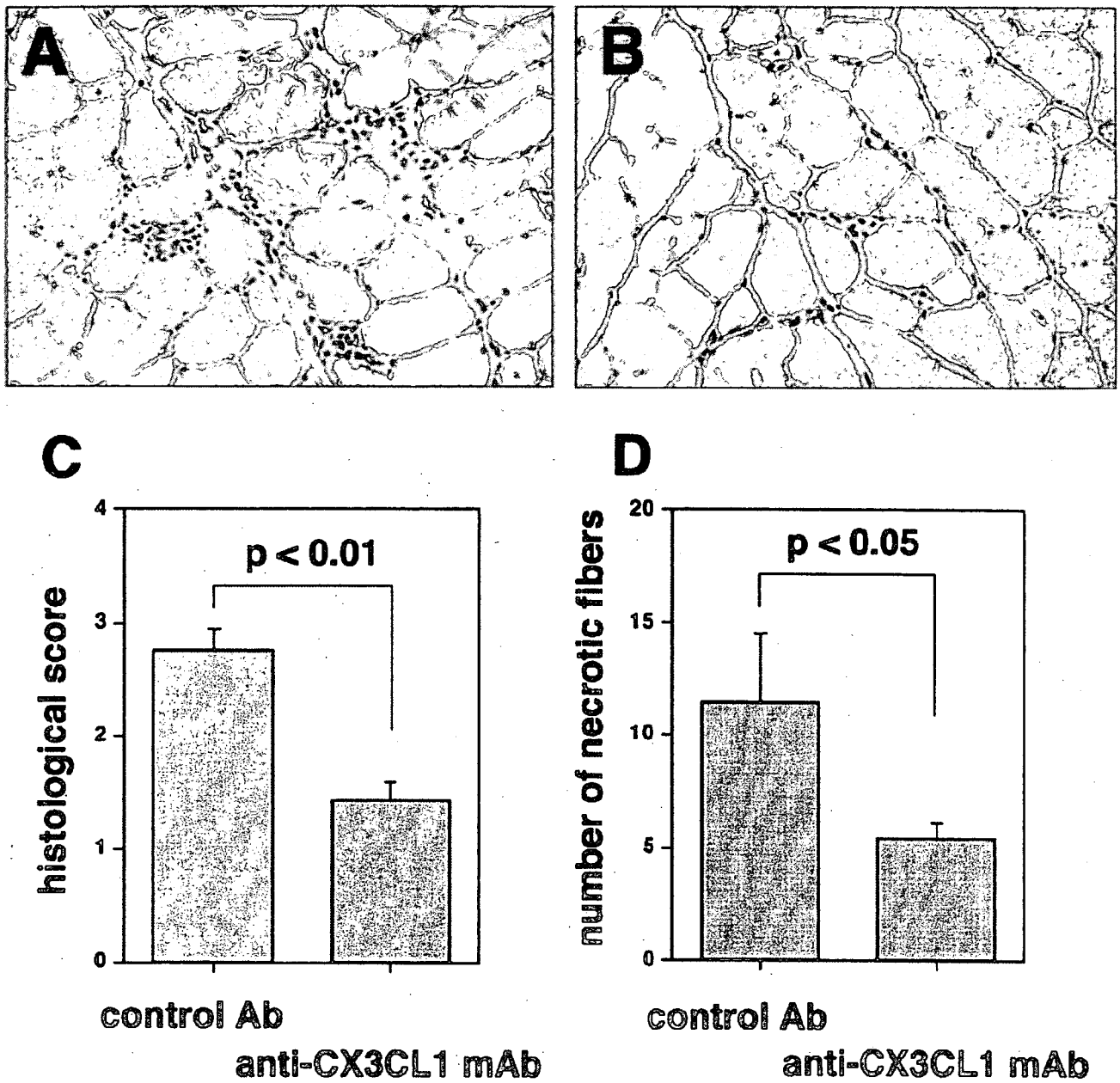

FIGURE 6. Inhibition of inflammatory changes in the muscle by treatment with anti-CX3CL1 mAb. Five hundred micrograms of hamster anti-mouse CX3CL1 mAb or control Ab was injected into the peritoneal cavity three times per week from day 0 for 3 wk. On day 21, the quadriceps femoris muscles of EAM mice were examined with H&E staining, histological scores were evaluated, and the numbers of necrotic fibers were counted. Mice treated with control Ab showed inflammatory cell accumulation (*A*). Mice treated with anti-CX3CL1 mAb showed milder inflammatory changes (*B*). Representative photomicrographs of histology from 10 animals in each group are shown. Histological scores of inflammatory changes in quadriceps femoris muscles were evaluated (*C*). The numbers of necrotic fibers were counted in the muscle tissues (*D*). Data represent the mean ± SEM.

(9–14). In the present study we focused on the role of CX3CL1-CX3CR1 interaction in the inflammatory cell migration. We showed the expression of CX3CR1 on some CD4 T cells and most CD8 T cells in EAM mice. It has been reported that CTLs including both $CD4^+$ and $CD8^+$ T cells invade the muscle fibers in IIM patients (3). These cells possess cytotoxic molecules, such as perforin and granzyme B, which are released into muscle cells (4, 5). Furthermore, type 1 cytokines, such as TNF-α and IFN-γ, were expressed in the inflammatory lesions of IIM patients (6–8). These findings suggest that the cytotoxic molecules and type 1 cytokines play important roles in the inflammatory lesions in IIM patients. In contrast, we reported previously that peripheral blood $CX3CR1^+$ T cells express cytotoxic molecules and type 1 cytokines (26, 27). Therefore, the interaction of CX3CL1 and CX3CR1 could induce the migration of T cells, which express cytotoxic molecules and type 1 cytokines, into the affected muscles.

The infiltrated macrophages into the affected muscle also express inflammatory cytokines (9, 41). They express TNF-α and IL-1β, which could stimulate T cells, macrophages, and

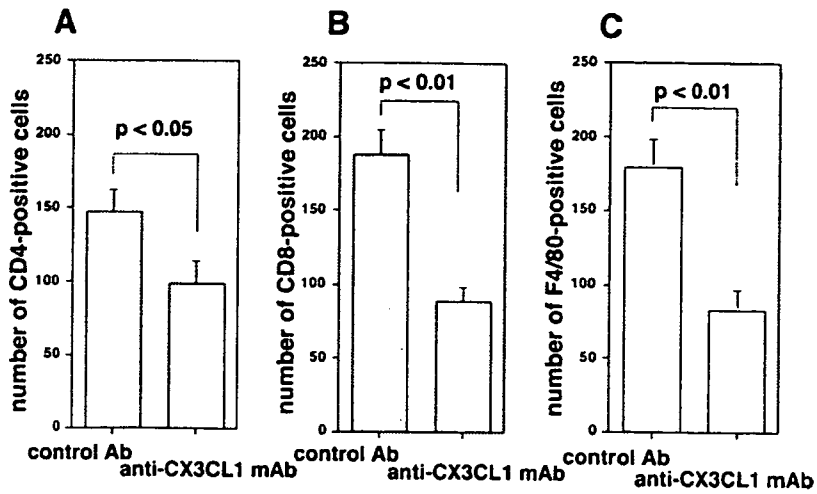

FIGURE 7. Decreased numbers of infiltrating cells of each subset by anti-CX3CL1 mAb treatment. Numbers of infiltrating $CD4^+$, $CD8^+$, and $F4/80^+$ cells were counted in the quadriceps femoris muscles from the experiment shown in Fig. 6. Data represent the mean ± SEM.

endothelial cells to produce various inflammatory cytokines, chemokines, and adhesion molecules. Moreover, these cytokines might have myocytotoxic effects (42–44). Our results showed that the majority of the $F4/80^+$ macrophages expressed CX3CR1 in the muscle of EAM mice. Thus, the CX3CL1-CX3CR1 interaction might also play an important role in macrophage migration into the affected muscle in addition to T cell migration.

CX3CL1 was expressed on infiltrated mononuclear cells in the affected muscles of EAM mice. Because CX3CL1 expression was located in the endomysium, infiltrated macrophages and/or CD8 T cells may express CX3CL1 in the muscles. Furthermore, we showed that CX3CL1 was also expressed on vascular endothelial cells in the EAM muscle tissue on days 14 and 21, but not in normal mice. It was reported that CX3CL1 was expressed on endothelial cells activated with TNF-α and IFN-γ in vitro (19–21). Expressed CX3CL1 on endothelial cells might recruit $CX3CR1^+$ cells, including macrophages and T cells, into muscle. These cells, in turn, express TNF-α and IFN-γ, which induce additional CX3CL1 expression on endothelial cells and also on recruited inflammatory cells. The enhanced expression of CX3CL1 may induce additional inflammatory cell migration. Consequently, these amplification cascades could contribute to the expansion of pathological changes in EAM mice. In fact, inhibition of CX3CL1 reduced the numbers of migrated CD4 and CD8 T cells and macrophages in the affected muscles of EAM mice and also reduced the expression of TNF-α, IFN-γ, and perforin. These results suggest that CX3CL1 blockade reduces the migration of inflammatory cells, which express cytotoxic molecules and cytokines, into the muscles. Thus, inhibition of CX3CL1-CX3CR1 interaction might be a potentially suitable therapeutic strategy for treatment of IIM.

Our data showed that mRNA expression of TNF-α, IFN-γ, and perforin was almost totally inhibited by anti-CX3CL1 mAb treatment, although the numbers of infiltrated monocytes were decreased by up to 50%. Recently it was reported that stimulation with CX3CL1 enhanced production of proinflammatory cytokines such as IFN-γ as well as the release of cytolytic granules by T cells (45). Thus, blockade of CX3CL1 might inhibit not only cellular migration, but also cytokine and cytotoxic molecule expression, by stimulation with CX3CL1 in the EAM muscle. Alternatively, because $CX3CR1^+$ T cells express type 1 cytokine and cytotoxic molecules (23, 26, 27), and $CX3CR1^{high}$ positive monocytes greatly produce inflammatory cytokines compared with $CX3CR1^{low}$ positive monocytes (46–48), treatment with anti-CX3CL1 mAb may selectively inhibit the migration of such specific T cells and macrophages. Therefore, anti-CX3CL1 mAb might be able to inhibit the expression of cytokine and cytotoxic molecules effectively in muscles, but additional study is required.

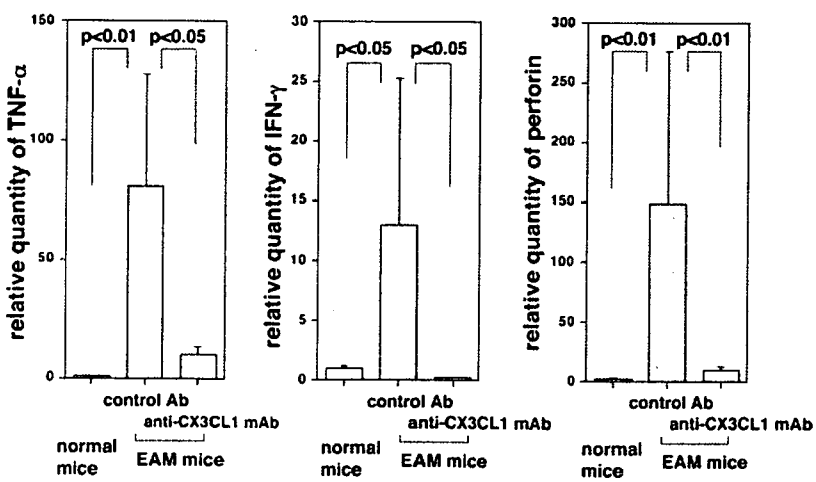

FIGURE 8. Reduction of TNF-α, IFN-γ, and perforin expression by anti-CX3CL1 mAb treatment. Expression of TNF-α, IFN-γ, and perforin mRNA in quadriceps femoris muscles from normal mice (n = 10) and from the experiment shown in Fig. 6 were measured using real-time RT-PCR. Data represent the mean ± SEM.